Marine and Petroleum Geology 143 (2022) 105812

Contents lists available at ScienceDirect

Marine and Petroleum Geology

journal homepage: www.elsevier.com/locate/marpetgeo

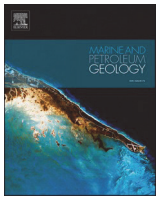

Structural inheritance in the Chukchi shelf, Alaska

Christopher D. Connors [a, b, *], David W. Houseknecht [b]

[a] Washington and Lee University, Lexington, VA 24450, USA
[b] U. S. Geological Survey, Reston, VA 20192, USA

ARTICLE INFO

Keywords:
Structural inheritance
Structural inversion
Hanna trough
Chukchi
Alaska

ABSTRACT

Interpretation of over 100,000 line-km of reprocessed 2D, time-migrated, seismic-reflection data from the U.S. Chukchi shelf documents at least four tectonic events in the last 400 m.y. that generated distinct inherited structures. A well stratified economic basement whose internal geometry clearly defines a pre-Mississippian, thin-skinned fold-and-thrust belt represents the earliest recognizable tectonism in the area, one that accommodated west-east (present-day coordinates) shortening, probably in the Devonian. (1) The first inversion event, and dominant crustal feature in the Chukchi shelf, is the Hanna Trough, a north-south, failed rift system that accommodated more than 10 km of Carboniferous-Jurassic syn-rift and post-rift (sag) strata. Carboniferous extensional collapse of the previous orogenic belt to form the Hanna Trough was influenced heterogeneously by the pre-Mississippian contractional fabrics. Many rift-phase normal faults detach along pre-Mississippian thrust faults in discrete negative inversion, creating distinctive synthetic growth strata that constrain the geometry of extension. Other normal faults cut across pre-Mississippian stratigraphy showing more typical rollover geometries in growth strata and dissection of contractional structures in the pre-rift strata in more distributed negative inversion. (2) After a period of Pennsylvanian to Early Jurassic subsidence, in the south-central Chukchi shelf several north-south, rift-phase normal faults were inverted in a second event in the Late Jurassic to Early Cretaceous, forming local, asymmetric, positive inversion structures due to west-east shortening likely associated with far-field effects of the Chukotkan orogeny. The Hanna Trough then was buried beneath >2 km of Cretaceous and Cenozoic foreland-basin deposits during which complex additional deformation occurred in the region. (3) The North Chukchi high resulted from Late Cretaceous-Paleogene deep thrusting, both south- and north-directed, and possible transpressional inversion across a complex older structural fabric. (4) Cenozoic east-west extension and strike-slip faulting in the northern Hanna Trough reactivated Carboniferous rift structures, in the west as dominantly discrete motion on the older faults, and in the east in more distributed fashion coalescing near older rifts and cutting Late Cretaceous-Paleogene contractional structures during a final negative inversion. Documentation of multi-phase structural inheritance in the Chukchi shelf is vital to unraveling the tectonic history and influences on petroleum systems in the area.

1. Introduction

The Phanerozoic tectonic history of the Chukchi shelf records a complex, multiphase history of deformation in Arctic Alaska. We document here the importance of structural inheritance in understanding this rich history. Located northwest of the Alaska North Slope, the U. S. Chukchi shelf comprises almost 200,000 km^2 with present-day bathymetry less than ~60 m. The area of interest is limited to the region north of the Herald Arch thrust system, east of the U. S. – Russia maritime boundary, south of the North Chukchi Basin, and west of the Alaska coastline (Fig. 1).

Previous work in the Chukchi shelf (Sherwood et al., 1998, 2002; Kumar et al., 2011; Homza and Bergman, 2019) link the stratigraphy of the Chukchi shelf to that of the better-studied North Slope, where four tectonostratigraphic megasequences are recognized (Lerand, 1973; Hubbard et al., 1987; Bird, 2001, Fig. 2). The Devonian and older Franklinian megasequence constitutes a transition from passive margin to foreland-basin sedimentation, culminating with significant fold-and-thrust belt development (Sherwood, 1994). The Mississippian-Triassic Ellesmerian megasequence documents a transition from continental rifting to form the Hannah Trough to passive margin and sag-basin development (Sherwood et al., 2002; Homza and

* Corresponding author. Washington and Lee University, Lexington, VA 24450, USA.
E-mail address: connorsc@wlu.edu (C.D. Connors).

https://doi.org/10.1016/j.marpetgeo.2022.105812
Received 20 October 2021; Received in revised form 23 June 2022; Accepted 27 June 2022
Available online 1 July 2022

Bergman, 2019). The Beaufortian megasequence represents a fundamental shift in tectonics in the area during Middle Jurassic-Early Cretaceous rifting and formation of the North Chukchi and Canada Basins (Hubbard et al., 1987; Houseknecht and Bird, 2004; Hutchinson et al., 2017; Homza and Bergman, 2019; Houseknecht, 2019a). The Brookian megasequence represents a change in provenance and foreland basin deposition from Early Cretaceous (Barremian-Aptian) on in response to Chukotka and Brooks Range orogenesis (Sherwood et al., 2002; Homza and Bergman, 2019; Houseknecht, 2019b; Lease et al., 2022). It is the tectonism associated with these megasequences, as well as superimposed Late Cretaceous-Cenozoic contraction and extension local to the Chukchi region, that drove the ubiquitous structural inheritance present in the Hanna Trough.

2. Structural inheritance

It is well known that older deformation can influence subsequent deformation. Implicit in this concept of structural inheritance is that events are temporally distinct with a period of inactivity separating episodes of deformation (Holdsworth et al., 1997). Perhaps the most straightforward type of inheritance is classic fault reactivation in which later fault movement is localized on older faults as a result of decreased material strength (Byerlee, 1978; Handy, 1989) and fluid reactions in the fault zone (Wintsch et al., 1995). This can occur at the individual fault scale through the crustal scale, such as along the Alpine fault in New Zealand, where multiple ages of deformation in the same zone have been documented (White and Green, 1986). Commonly, interactions with pre-existing fabrics act to nucleate later deformation in a more distributed fashion, such as the influence of late Paleozoic basement fabrics on Cenozoic rifts in the Upper Rhine Graben in Germany (Schumacher, 2002).

Structural inversion (Glennie and Boegner, 1981; Bally, 1984; Cooper and Williams, 1989; Buchanan and Buchanan, 1995) constitutes a particular type of structural inheritance whereby the sense of motion on faults, generally dip-slip, changes over time. While a period of tectonic quiescence is not mandatory, a change in far-field stress is required. The archetype example of inversion on discrete structures occurs as reverse faulting along earlier normal faults. This reactivation forms distinctive asymmetric fault-related folds with long back limbs and short front limbs (Williams et al., 1989). In the extreme, these inverted structures can be so asymmetric that the front limbs are thought of as distinct structures separate from the basement uplift, such as the monoclines in the Colorado Plateau, even though they are clearly tied to the overall, larger contractional uplift (Bump, 2003). Structural inversion is not simply conceptualized within the context of individual structures but also on a regional scale (Tari et al., 2020), for example, the full basin inversion of the Uinta Mountains during the Laramide orogeny (Hansen, 1986). Likewise, it is well known that the many older

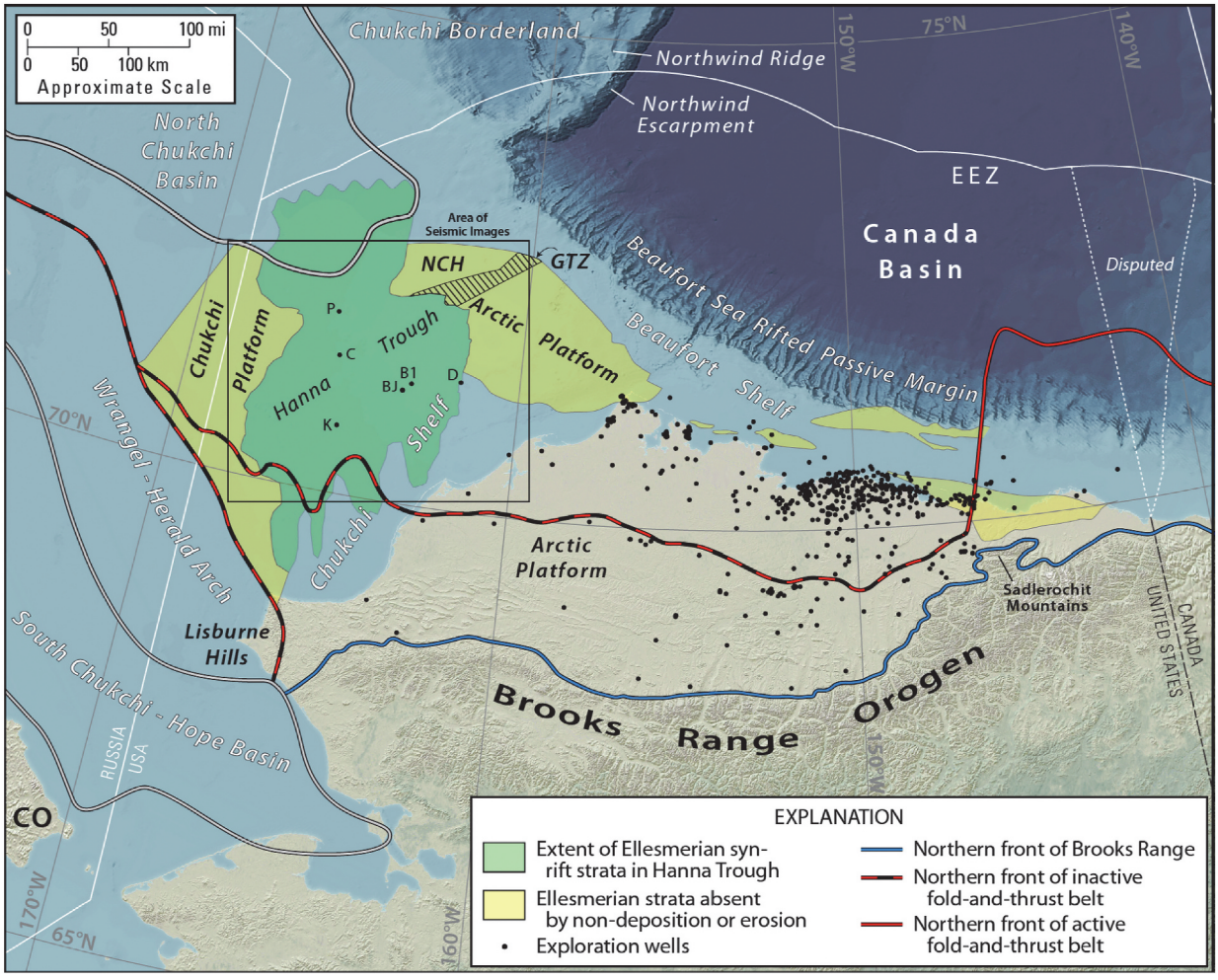

Fig. 1. Location of the Chukchi shelf and adjacent onshore. Approximate locations of seismic lines shown in paper are within the box as follows: Figs. 4 and 11 E-W line in the north-central; Fig. 5 E-W lines in the east-central; Fig. 9 E-W line in the southwest; Fig. 10 N–S line in the north-central. North Chukchi high (NCH); Grantz transpressional zone (GTZ); Exclusive Economic Zone (EEZ); Chukotkan orogen (CO); wells Popcorn (P), Crackerjack (C), Klondike (K), Diamond (D), Burger (B1), Burger J (BJ).

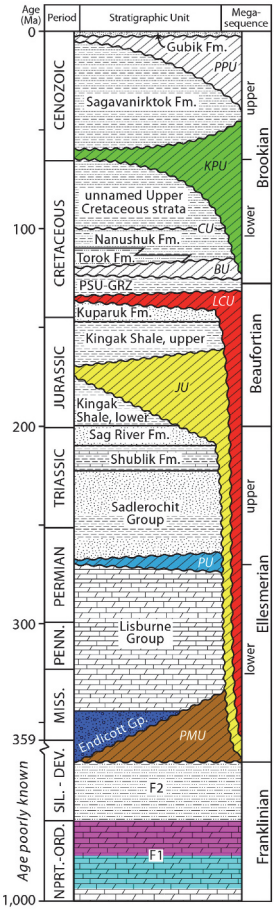

Fig. 2. Chronostratigraphy of the Chukchi shelf, modified from Craddock and Houseknecht (2016). Franklinian, lower part (F1); Franklinian, upper part (F2); pre-Mississippian unconformity (PMU); Permian unconformity (PU); Jurassic unconformity (JU); Lower Cretaceous unconformity (LCU); Brookian unconformity (BU); Cenomanian unconformity (CU); Cretaceous-Paleogene unconformity (KPU); Pliocene-Pleistocene unconformity (PPU). Colored unconformities and strata keyed to horizons of same color in figures of seismic images. (For interpretation of the references to color in this figure legend, the reader is referred to the Web version of this article.)

rift basins form the loci of later orogenic belts, such as in the Pyrenees (Muñoz, 1992; Teixell et al., 2018). In these cases, attenuated continental crust serves to focus later contraction (Jackson, 1980). Whether at the local or regional scale, the later uplift in strata above a regional datum was termed positive inversion by Glennie and Boegner (1981).

In contrast, negative inversion (Glennie and Boegner, 1981) is the result of early contraction followed by later extension, resulting in subsidence below a regional datum. This is less commonly documented in the literature for discrete structures, perhaps because older thrust faults generally are not at a favorable orientation to resolve significant shear stress during later extension. Imbrication associated with thrust belts however can cause faults to steepen and thus be in more favorable orientations for later changes in the far-field stress (Tari et al., 2021). At the largest scale the concept of negative inversion encompasses extensional orogenic collapse (Dewey, 1988) due to crustal thickening that causes the lower crust to weaken and act as a region of later crustal extension. In some mountain belts detachment horizons in extension likely reactivate older contractional detachments. This is well documented in mountain belts such as the Cenozoic Cordillera of North America (Bally et al., 1966; Constenius, 1996). Repeated inheritance with different structural styles has been recognized in certain mountain belts, such as the control that the extensional Mesozoic Montmell fault in the Catalan Coastal Range, Spain had on Paleogene contractional and Neogene extensional fault systems (Marín et al., 2021). Similarly, basement structures have been shown to be reactivated multiple times, such as in offshore Norway (Phillips et al., 2016).

There are several ways to identify structural inheritance in seismic reflection data. 1) As discussed above, multiple periods of motion on faults, whether inverted or simply reactivated, are a clear indication of structural inheritance. Coupled with growth strata and multiple unconformities, these are unambiguous indicators of multiple events or styles. A particularly compelling example is the concept of a null point in positive inversion structures, below which there is a normal sense of throw, and above a reverse sense (Williams et al., 1989). 2) Map-view deformational patterns of different ages that have parallel trends are suggestive of reactivation. Holdsworth et al. (1997) termed these "geometric similarity" inheritance, and point out that when such parallelism of orientation is solely used they may not be reliable indicators of reactivation. Nonetheless, this criterion is useful when orientations with clear spatial overlap are used in conjunction with documented local reactivation of structures to extrapolate to a regional extent of reactivation. 3) Less obvious, but useful for recognition of inversion, are distinctive fault and fold geometries in cross section that differ from expected style. These shapes include the asymmetric positive inversion folds, but also, low-angle, steepening-bend normal faults that occur with negative inversion structures. The utility of these geometries is elaborated on later. Again, these are indirect indicators, and some independent temporal constraint is needed, such as growth strata or unconformities, to document multiple events regionally.

We show that every type of structural inheritance outlined above has occurred in the Chukchi Sea area over its complex Phanerozoic tectonic history. We use several seismic-reflection profiles to demonstrate that the tectonic evolution and present tectonic features of the area are better understood within the context of structural inheritance, both at the scale of individual structures and at the broader, basin scale. This framework is relevant to petroleum exploration in this underexplored area, as well the tectonics of the Arctic in general.

3. Database and methods

This report summarizes selected results from a regional seismic interpretation and mapping study of the subsurface of Arctic Alaska conducted over several years. Approximately 100,000 line-km of reprocessed 2D, time-migrated, seismic reflection lines constitute the primary data available for the Chukchi shelf. Well control is from six exploration wells (Fig. 1), with the deepest penetrated strata the Carboniferous Lisburne Group of the Ellesmerian megasequence (Fig. 2) in the Popcorn, Crackerjack, and Diamond wells (Sherwood et al., 2002). Thus, regional ties to deeper strata have relied on a broader, integrated, regional study of subsurface data that includes the North Slope and Beaufort Sea shelf. In the Arctic Alaska region, data availability includes several 100,000 line-km 2D, and 19 regional 3D seismic datasets, along with hundreds of exploration wells, including nearly 100 penetrations of the pre-Mississippian Franklinian megasequence (Fig. 3). These provide indirect constraints on pre-Mississippian strata in the Chukchi region.

Regional interpretation was conducted using standard seismic interpretation methods with particular emphasis on regional unconformities. Our nomenclature for these is similar to that of Homza and Bergman (2019), with slight modifications and simplifications. The pre-Mississippian unconformity (PMU), marking the top of the Franklinian megasequence delineates inferred pre-Mississippian strata and potentially igneous and metamorphic rocks from younger strata. This surface may contain uppermost Devonian strata above it, but for simplicity we chose to refer to this as the PMU, with analogy to the well penetrations on the North Slope and Beaufort shelf (Fig. 3), where no known pre-Mississippian strata sit above this regional unconformity. The Permian unconformity (PU) defines the top of the lower Ellesmerian megasequence, and the Jurassic unconformity (JU) marks

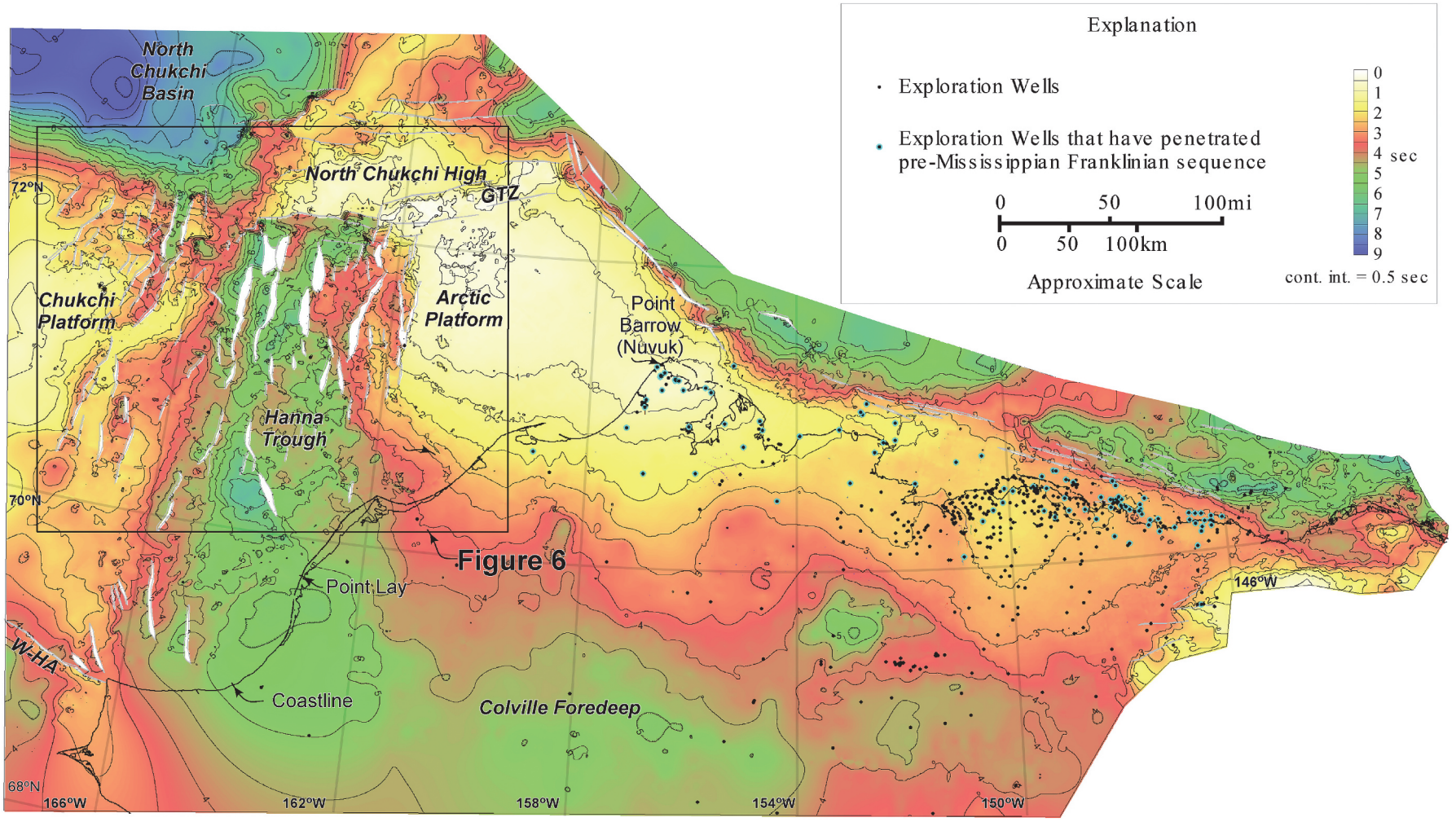

Fig. 3. Time-structure map of the pre-Mississippian unconformity in the Chukchi and Beaufort shelves and North Slope, Alaska. The Hanna Trough is clearly visible as the large north-south depression between the Chukchi and Arctic Platforms. Grantz transpressional zone (GTZ), Wrangel-Herald Arch (W-HA). Fault gaps shown in white.

approximately the top of the upper Ellesmerian megasequence but also comprises part of the lower Beaufortian. The Lower Cretaceous unconformity (LCU) is established nearly at the top of the Beaufortian megasequence. The Cretaceous-Paleogene unconformity (KPU) separates Cretaceous and Tertiary strata (Fig. 2). In places, erosion has resulted in composite unconformities, which cut through multiple megasequences. For example, the PMU shown in Fig. 3 represents the top of the Franklinian megasequence, even though on parts of the Chukchi and Arctic Platforms, Brookian strata rest directly on Franklinian and thus that surface also represents the LCU and all older unconformities at these locations. Key mapping surfaces tied to wells, where penetrated, and correlated in seismic data throughout the Chukchi shelf include these five regional unconformities shown in Fig. 2, the approximate top of the Endicott Group in the lower part of the Ellesmerian megasequence, and the base and top of an acoustically distinct succession in the lower part of Franklinian megasequence. Details of diagnostic criteria for these horizons are discussed below.

In addition to interpreting offset reflectors, faults were recognized using the principles of fault-related folding (Suppe et al., 1992; Xiao and Suppe, 1992; Shaw et al., 1997, 2005). These principles recognize fault-cutoff geometries and defined dip domains (regions of homogenous dip) to delineate fold geometries. From these the underlying fault geometries can be inferred that are compatible with fault-related folding equations, and thus structural balancing concepts. Parts of some complex, inherited structures were modeled with the program fbfFor (Connors et al., 2021), which follows the principles of fault-bend folding to produce balanced, kinematic, sequential forward models. The concepts of structural inheritance outlined above, namely the sense of fault offset on multiple horizons, analysis of growth strata and unconformities, regional map patterns, and diagnostic structural styles, were used to infer multiple deformation episodes.

With the exception of Fig. 4, seismic images are shown with approximately no vertical exaggeration for the deeper reflective section, which is the main focus of this report. The average seismic velocity in the Chukchi shelf for the deeper section is approximately 4400 m/s TWTT, based on Grantz et al. (1994) and proprietary industry data. Images displayed with a time axis shown with this average velocity will in general approximate a 1:1 section for the deeper section. Such displays have internal deviations from this, and will likely be modestly vertically exaggerated in the shallower section (up to ~1.5:1), but result in time sections that are as close as possible to undistorted. This allows for a more accurate representation of the true structural geometries depicted in these data, in order to understand the complex deformation present. Lateral velocity variations are generally gradual in the Chukchi shelf. One exception is a minor salt diapir west of the Popcorn well, where pullup is present in the time-migrated section as displayed in Fig. 4 at offset 90 km.

4. Neoproterozoic-early Paleozoic passive margin development, and Devonian folding and thrusting

A seismic transect across the central Chukchi shelf (Fig. 4) shows that shallower reflectors are mainly continuous across the shelf, whereas deeper reflectors truncate against a less reflective section in angular discordance. In the Chukchi Platform and central Hanna Trough, a prominent, deep reflector separates a weakly reflective to seismically quiescent section from an overlying clearly reflective section. We interpret this as the PMU at the top of the Franklinian megasequence, based on seismic similarity and many well ties to that unconformity beneath the North Slope and Beaufort shelf (e.g., Houseknecht and Connors, 2016). Major structural features of the region are shown in a time surface of the PMU in Fig. 3. These features include the Hanna Trough, a substantial structural low bounded by adjacent highs, the Chukchi Platform to the west, the Arctic Platform to the east, and the North Chukchi high to the north. The present-day depression of the PMU within Hanna Trough grades to the south into the Colville foredeep, a

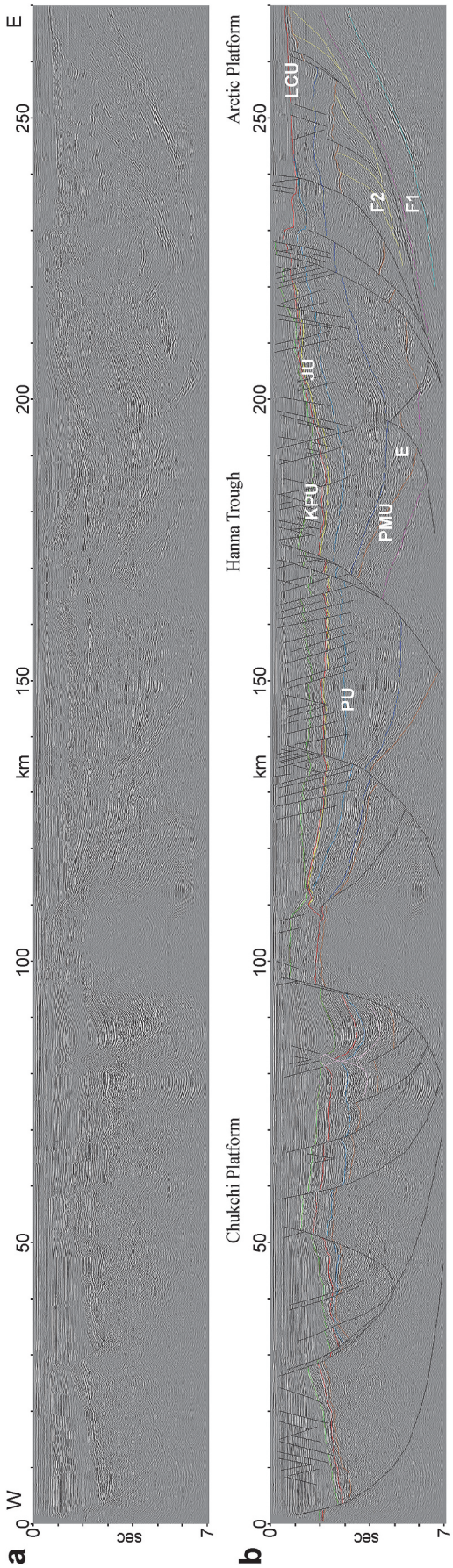

Fig. 4. Regional seismic transect across northern Hanna Trough shown with an approximately 2:1 vertical exaggeration for the deeper reflective section. See Fig. 1 for location. Franklinian, lower part (F1); Franklinian, upper part (F2); pre-Mississippian unconformity (PMU); Endicott Group equivalent (E); Permian unconformity (PU); Jurassic unconformity (JU); Lower Cretaceous unconformity (LCU); Cretaceous-Paleogene unconformity (KPU). a) Uninterpreted section. b) Interpreted section showing overall rift geometry to Hanna Trough, with multiple stages of complex structural inversion. See Fig. 11 for an enlarged version of the same seismic line and details of the deformation.

structural low associated with the Cretaceous-Paleogene Brookian orogeny (Houseknecht, 2022). Homza and Bergman (2019) defined the Hanna Trough with respect to the limit of the syn-rift Carboniferous Endicott Group. This corresponds to the structural highs listed above, and extends to the south to a latitude of approximately Point Lay (Fig. 3; Homza and Bergman (2019) their Fig. 10).

While the PMU is the deepest surface that can be unambiguously mapped regionally, deeper reflectors are observed locally, and these inform interpretations of the early tectonic history recorded in the Chukchi shelf. The deepest strata that can be correlated beyond individual seismic lines form a nearly isopachous succession defined by two moderate-to high-amplitude reflectors at the top and base in an otherwise transparent to low-amplitude succession on the east side of the transect shown in Fig. 4 (east of offset 220 km). No well penetrations of this succession are known and Grantz et al. (1982) interpreted it as sedimentary or metasedimentary strata based on lateral reflector continuity and postulated it to be early Neoproterozoic-Paleozoic in age (their "PzpCs Unit"). Craig et al. (1985) inferred this section to be carbonate based on seismic velocities and Embry (1990) suggested it to be correlative with Neoproterozoic-lower Paleozoic strata, dominantly carbonate shelf facies, of the Franklinian Basin in the Canadian Arctic Islands (Fox, 1985; Harrison and Bally, 1998; Harrison and Brent, 2005; Dewing et al., 2019). Sherwood (1994) invoked a similar correlation based on seismic similarity (his "Carbonate Unit"), as did Homza and Bergman (2019; their "Undeformed Carbonate Unit"). Kumar et al. (2011) referred to distinct reflectors in this section as "Intra-Franklinian reflectors D, E and F." Because neither the age nor lithology is definitively known, we refer to this succession as simply the F1 section, indicating its lower stratigraphic position in the Franklinian megasequence (Fig. 4). Although apparent stratigraphic reflectors locally are evident below F1 (Fig. 5), we observe no definitive stratal patterns and make no attempt to interpret the age or origin those older rocks.

Grantz et al. (1994) noted that the distinctive F1 section appears to continue into the western Beaufort shelf, east of Point Barrow (Nuvuk). Our correlations are consistent with this and suggest the succession is truncated by Mesozoic rift structures in the Beaufort shelf and may be present farther north and west as attenuated and dismembered blocks. The F1 section can be correlated throughout the Arctic Platform of the Chukchi shelf, the Northeast Chukchi Basin of Grantz et al. (1994), and west into the center of the Hanna Trough. Notably, we do not recognize it in the Chukchi Platform west of the Hanna Trough (Fig. 4) where reflectivity is poor.

We concur with previous authors that this several-km thick F1 section may be correlative with Neoproterozoic-lower Paleozoic strata in the Canadian Arctic Islands and further suggest it may be equivalent to the Neoproterozoic Katakturuk Dolomite and lower Paleozoic Nanook Group platformal succession exposed in the Sadlerochit and Shublik Mountains (Macdonald et al., 2009; Strauss et al., 2013, 2019). Thus, we suggest the F1 section may plausibly represent a Neoproterozoic through Ordovician, or possibly even Lower Devonian, passive margin succession in the Franklinian megasequence in the Chukchi shelf.

Overlying F1 is a well stratified section that displays discontinuous reflector packages of consistent dip, separated by sharp breaks in dip across interfaces, some of which are flat and others that are dipping (Fig. 5). These dip domains, which commonly display irregular geometry (Fig. 5d), generally flatten to approach the dip of the underlying F1 at depth and are truncated by the PMU (Fig. 5c). Complicating interpretation of this interval are shallowly dipping, conflicting seismic events cutting across other events, such as at offset 87–100 km in Fig. 5a. Because these mimic shallower reflectors, we interpret these as multiple reflections from shallower interfaces.

This section has not been penetrated by wells on the Chukchi shelf, and because of the discontinuous character cannot be clearly tied to penetrations in the North Slope or Beaufort shelf. This section has been interpreted as siliciclastic strata (Craig et al., 1985; Sherwood, 1994) that may be Early to Middle Devonian in age, based on similarity to the Ellesmerian foreland basin clastic wedge in the Canadian Arctic Islands (Miall, 1976; Embry, 1991; Harrison and Brent, 2005; Beranek et al., 2010). Alternatively, the section, particularly the lower part, may be Silurian flysch analogous to that found in the northern Canadian Arctic Islands (Trettin, 1998; Hadlari et al., 2014; Dewing et al., 2019) because the docking of Pearya in the Canadian Arctic Islands is thought be Late Ordovician to early Silurian (Trettin, 1998; McClelland et al., 2012). The F2 section may also be composed of foreland-basin deposits associated with the Arctic Caledonian orogeny which may have continued into the Early Devonian in the Chukchi borderland (O'Brien et al., 2016; Miller et al., 2017). The closest wells to the Chukchi study area that penetrate pre-Mississippian strata are those on the North Slope near Utqiagvik (formerly Barrow), where Upper Ordovician to Silurian rocks have been penetrated (Carter and Laufeld, 1975; Dumoulin, 2001; Houseknecht and Connors, 2016). Thus, we conclude that this reflective section in the Chukchi shelf is Late Ordovician-Devonian in age and denote it as the upper Franklinian F2 section.

Our interpretation of the F2 section is that it experienced significant contractional deformation, consistent with the interpretations of Sherwood (1994) and Homza and Bergman (2019). Because of the intense deformation, the large spacing of the 2-D seismic grid available, and the lack of distinctive reflectors in this section, we did not attempt to correlate across all thrust sheets, but instead used fault-related folding principles (Shaw et al., 2005) to constrain structural style and fault and fold geometries locally. Specifically, we interpret the predominately west-dipping domains that are truncated locally as west-dipping thrust sheets cutoff against adjacent thrusts (Fig. 5). These geometries are consistent with contractional, imbricate fault-bend folding (Shaw et al., 2005) indicative of a dominantly eastward vergence and tectonic transport direction. Houseknecht and Connors (2016) recognized similar geometries in reflectors they interpreted to be Franklinian in the Beaufort shelf. We interpret the deformation to be detached at the base of the imbricated Upper Ordovician-Devonian strata because of the absence of these dip panels in the inferred Neoproterozoic-lower Paleozoic passive margin succession (F1, Fig. 5). In places, some intermediate detachment horizons likely are present in F2, with associated front limbs preserved, but several of the thrusts appear to have ramped to a paleosurface, or were later eroded (Fig. 5a and b). The clear angular truncations with the overlying reflectors suggest erosion of the thrust sheets, and the formation of local angular unconformities at the PMU. The irregular nature of this surface may be a relict topography recorded on the top of the fold-and-thrust belt (Fig. 5c).

No contractional growth strata are observed in the F2 interval. If an Early Devonian depositional age is correct for F2 and because the pre-Mississippian unconformity separates the Ellesmerian megasequence from the Franklinian megasequence below, then folding and thrusting are plausibly Middle to Late Devonian. As with the F1 succession, the fold-and-thrust belt is predominantly recognizable in the Arctic Platform, and can be mapped as far west as the center of the Hanna trough, but not west into the Chukchi Platform (Fig. 6a). The poor reflector character to the Franklinian megasequence in the Chukchi Platform suggests highly deformed, steeply dipping beds, and potentially an igneous or metamorphic component to the rocks. Subsequent rifting, discussed below, commenced in the Early Mississippian, substantially modifying and obscuring the older fold-and-thrust belt geometry.

5. Mississippian negative inversion

Seismic events above the PMU are highly reflective, and locally, in the deepest positions, display dips that fan to steeper dips at greater time (e.g., Fig. 4, in the center of the Hanna Trough). These generally abut moderately dipping interfaces, and locally in their upper extents are angularly truncated against flat-lying to gently dipping reflectors (e.g., Fig. 5d, offset 65 km). We interpret these intervals as expanded lower part of the Ellesmerian growth strata (Endicott Group) in half grabens above mostly west-dipping normal faults in the center and eastern parts

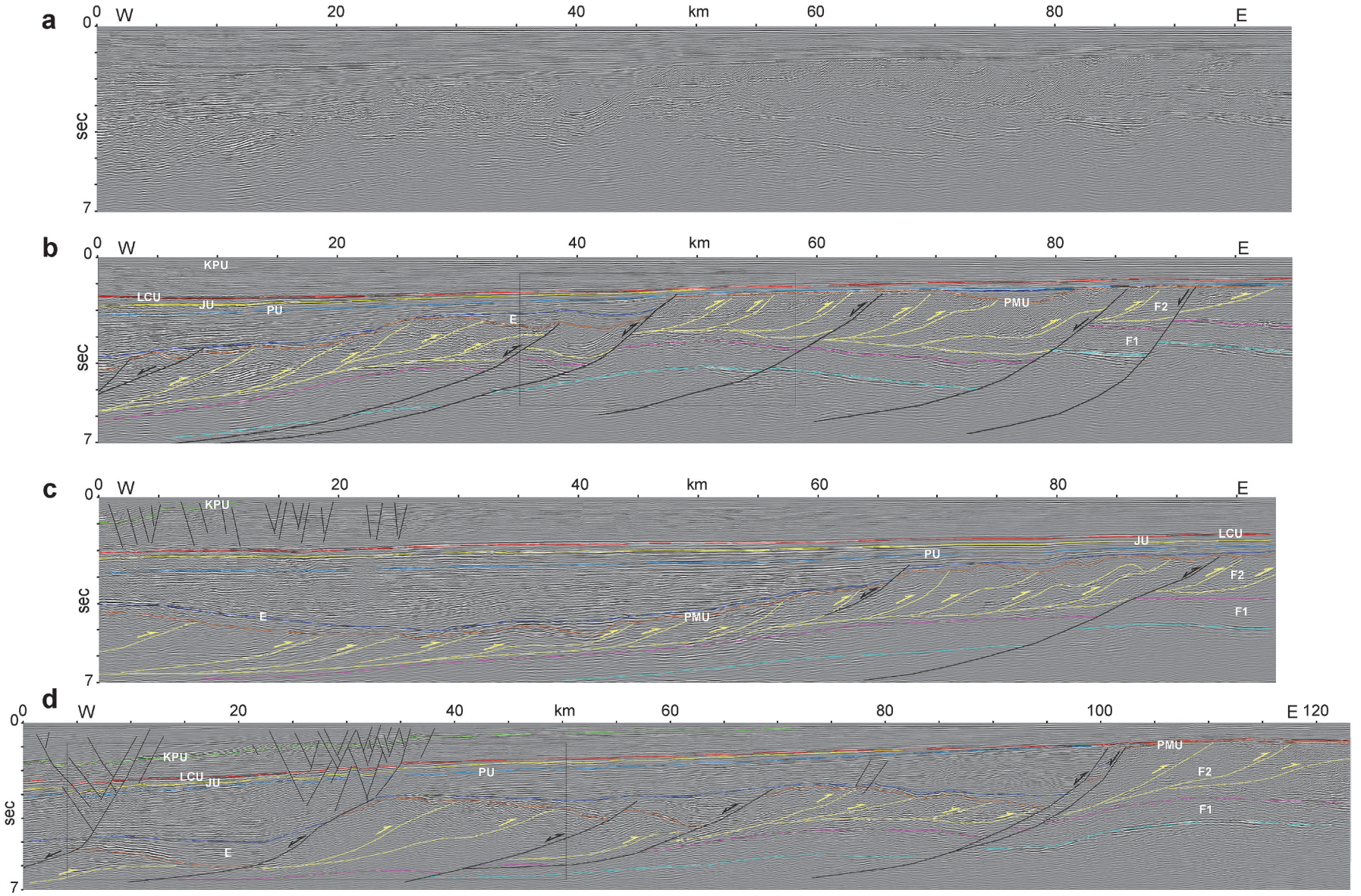

Fig. 5. Seismic lines straddling the eastern Hanna Trough and western Arctic Platform. See Fig. 1 for locations. A Devonian thin-skinned fold-and-thrust belt involving the Franklinian F2 strata, detaches above the flat-lying Franklinian F1 section. Subsequent Mississippian-Pennsylvanian crustal extension was influenced by the Devonian contractional structures in a variety of ways. Franklinian, lower part (F1); Franklinian, upper part (F2); pre-Mississippian unconformity (PMU); Endicott Group equivalent (E); Permian unconformity (PU); Jurassic unconformity (JU); Lower Cretaceous unconformity (LCU); Cretaceous-Paleogene unconformity (KPU). a) Uninterpreted seismic section. b) Interpreted seismic section of (a) showing Mississippian crustal extension in negative inversion along older thrust fault in the center of line. Crustal normal faults cut older contractional detachment surface on the east side of the line. Box indicates region modeled in Fig. 7 c) Interpreted seismic section showing pre-Mississippian unconformity has an undulating residual topography that records the top of the fold-and-thrust belt. d) Interpreted seismic section showing Mississippian-Pennsylvanian crustal extension on the west side of the line. Motion on this normal fault took advantage of older, contractional detachment at depth to form distinctive synthetic rollover geometry to extensional growth strata. Box indicates region modeled in Fig. 8. Other rift-related normal faults interact with pre-existing contractional structures to form complex, truncated geometries and buttress unconformities.

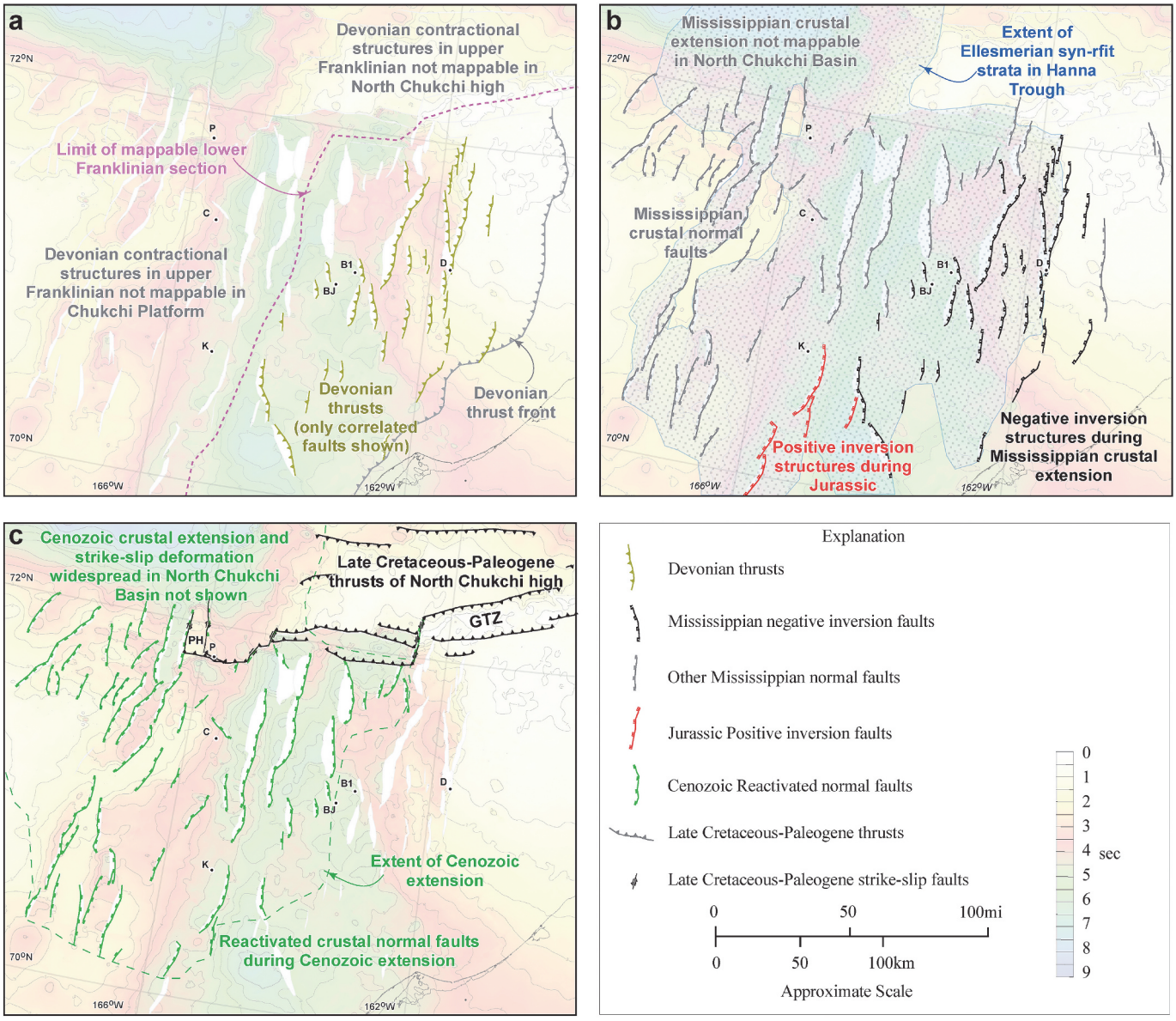

Fig. 6. Maps of correlated large faults active at different times in the Chukchi shelf, showing the importance of structural inheritance. Location is shown as box in Figs. 1 and 3. Underlying map is the pre-Mississippian unconformity time surface from Fig. 3. Grantz transpressional zone (GTZ), Popcorn high (PH); wells Popcorn (P), Crackerjack (C), Klondike (K), Diamond (D), Burger (B1), Burger J (BJ). a) Devonian contractional structures in the Hanna Trough and Arctic Platform. b) Mississippian rift-related extensional structures, including negative inversion structures, and Jurassic positive inversion structures in the Hanna Trough and Arctic Platform. c) Late Cretaceous-Paleogene contraction in the North Chukchi high and reactivated Cenozoic extensional structures in the Hanna Trough and Chukchi Platform.

of the trough (Fig. 4). These structures define the dominant structural feature in the Hanna Trough, a north-south, failed rift system. Crustal extension is proposed to have commenced in the Late Devonian (Sherwood et al., 2002; Homza and Bergman, 2019). Because this section has not been penetrated in the Chukchi shelf, the age of the onset of rifting is poorly constrained, but likely was occurring by the Early Mississippian, potentially extending into the Pennsylvanian.

Lying above the growth strata, flat-lying to gently dipping, continuous reflectors are present, tied to well penetrations in the Ellesmerian Lisburne Group (Sherwood et al., 2002). This section locally truncates against steeply dipping reflectors at high angles (e.g., Fig. 5c, offset 65–67 km). We interpret these as upper Carboniferous Lisburne strata pinching out against bathymetric scarps, thereby forming buttress unconformities. These likely mark the cessation of rifting and onset of a sag-basin phase (Homza and Bergman, 2019). There may have been continued minor extension during deposition of Lisburne Group strata because the geometry of strata in this section against scarps is not entirely flat-lying in places, such as can be seen on the east of the Hanna Trough (e.g., Fig. 5d, offset 100–103 km).

Fanning, antithetic dip (rollover) in half grabens is commonly observed and associated with syntectonic (growth) strata related to displacement on flattening normal faults (Xiao and Suppe, 1992; Shaw et al., 1997; and many others). Other evidence for the flattening of many of these faults into a mid-crustal detachment zone is indicated by the structural relief across half grabens where the syn-rift lower Ellesmerian section shows little structural relief across hinges. That is, this relationship suggests that only heave could be accommodated at these positions away from the steeper fault segments, based on area balancing constraints. We interpret the northern part of the Hanna Trough to comprise multiple, flattening normal faults that dip both east and west, based on the constraints outlined above. The main rift geometry and timing interpreted here are broadly consistent with previous

interpretations by Sherwood et al. (2002), Kumar et al. (2011), and Homza and Bergman (2019). The greatest throw on these crustal normal faults is more than 4 s TWTT on several west-dipping faults (Fig. 4, offset 160 km). Based on typical seismic velocities in the area, we estimate that more than 8 km of syn-rift and post-rift Carboniferous section is preserved in these half grabens. Crustal normal faults are present in the Chukchi and Arctic Platforms, but because of later uplift and erosion do not preserve syn-rift strata (Fig. 6b).

The Hanna Trough demonstrates clear reactivation and inversion as indicated by growth strata, local unconformities, and distinctive fault-related folding geometries. In this section we focus on the first of these events related to Carboniferous rifting. In subsequent sections we discuss the later events, and the role of structural inheritance in their development. The Carboniferous rift-related faults generally offset the entire Franklinian section, and typically cut below the Devonian contractional detachment level (Fig. 5). The presence of pre-F1 high-angle faults, evidenced by expanded reflectors below F1 in Fig. 5a and b at offset 85–90 km, may explain why some Carboniferous faults cut the entire basement section. We suggest this evidence represents growth associated with a pre-F1 rift-related fault that provided a zone of weakness reactivated during Carboniferous rifting.

Nonetheless, at shallow levels the Carboniferous normal faults generally appear to localize on or near older thrusts in the F2 section. The reason for this shallow reactivation is likely because these thrusts are commonly imbricated and are steeper than primary thrust faults. Thus, they would have been in a more favorable orientation to slip in negative inversion when the stress field changed to one where crustal extension dominated; that is, where the maximum compressive stress was close to vertical. The fact that these normal faults also generally cut the older F2 contractional detachment horizon suggests that this surface was not as weak as the heterogenous (and commonly previously faulted) mid-crust during Carboniferous rifting.

The structures in Fig. 5a and b shows examples of this relationship of shallow negative inversion of Devonian thrusts, with offset of the detachment horizon and shallowly dipping F1 at depth. A compelling example is the complex structure imaged in the highlighted box on Fig. 5b. The seismic energy here is strong, with clear reflectors and few

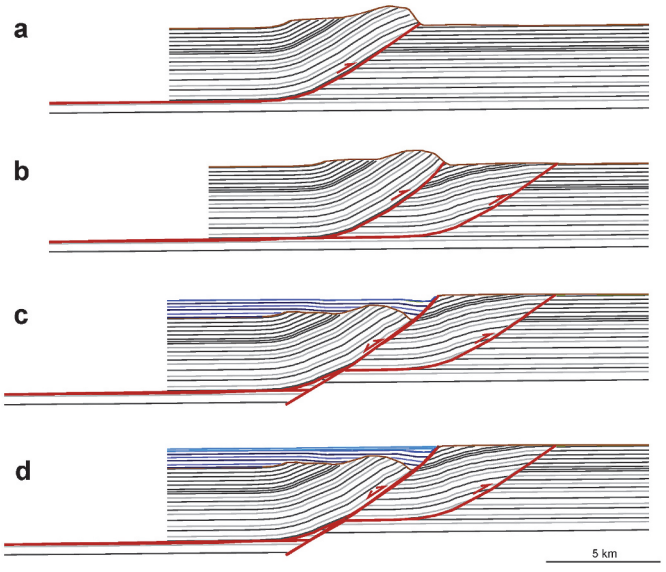

Fig. 7. Balanced sequential forward model of the negative inversion structure shown in the inset box of Fig. 5b. a) and b) a break-forward imbricate Devonian fold-and-thrust belt develops and is eroded, causing the steep dip to the F2 section, and an angular truncation at the PMU. c) Carboniferous extension reactivates one of the thrust planes in negative inversion and offsets the detachment and F1 section at depth. d) post-extension sedimentation fills in the accommodation created by the extension.

conflicting or cross-cutting reflectors. Thus, we believe the section has been migrated well, and is indicative of true, complex structural geometry. These same relationships are present along strike in other seismic lines, providing further confidence in the relationships inferred on this structure. The geometry is one in which the hanging wall shows steep, west-dipping reflectors of the F2 section in angular truncation with a shallow, predominantly east-dipping lower part of the Ellesmerian section. Furthermore, there is a relict topography on the PMU unconformity. The F2 section dips west in the hanging wall, close to the dip of the Carboniferous normal fault. In the footwall, the F1 is nearly horizontal. A possible explanation of this odd geometry is shown in the sequential, balanced, forward, kinematic model of Fig. 7. The seismic section is not depth-migrated, and thus the model is not meant to exactly replicate the seismic section. Nonetheless, the model satisfactorily explains the observed seismic geometry in the Carboniferous and older section. The model steps shown in Fig. 7a and b illustrate a break-forward, imbricate Devonian fold-and-thrust belt with steep westward dip and subsequent angular truncation by the PMU. Fig. 7c is a model step showing how Carboniferous extension reactivated one of the thrust planes in negative inversion but did not follow the thrust plane down to a detachment, but rather flattened slightly at the older flat-ramp transition and offset the detachment and F1 section at depth. Sedimentation occurred in the accommodation created by the extension (Fig. 7c and d) with gentle antithetic dip into the fault. Had the normal fault flattened to the contractional detachment and formed a large concave bend, and assuming the lower part of the Ellesmerian section was syn-rifting, there should have been significant antithetic rollover into the fault based on extensional fault-bend folding theory (Xiao and Suppe, 1992; Connors et al., 2021). This reactivated fault coalesces with another rift-related fault just to west (Fig. 5b) and gently flattens into the center of the Hanna Trough. As discussed above, in other places in the Hanna Trough more pronounced antithetic rollover is observed for many of the large half grabens related to a mid-crustal detachment (Fig. 4).

Another unusual structural geometry related to Carboniferous negative inversion is shown in the highlighted box in Fig. 5d. At this locality near the center of the Hanna Trough, Endicott Group strata are generally deeper than 5 s TWTT (offset 7–27 km) and display bidirectional dip and thicken into a syncline. On the east flank of the syncline, the lower part of the Ellesmerian strata thin and pinch out by onlap onto an inferred, west-dipping Carboniferous normal fault. Although east-dipping strata on the west flank of the syncline are consistent with antithetic rollover on a flattening normal fault, west-dipping strata on the east flank suggest synthetic rollover relative to the normal fault. These observations are consistent with extensional fault-bend folding theory of a convex, extensional fault-bed (Xiao and Suppe, 1992; Connors et al., 2021). Fig. 8 demonstrates a sequential, balanced, forward, kinematic model that explains this observed Carboniferous and older geometry. The model is not an exact attempt at matching the observed structure, and the absence of post-Carboniferous differential subsidence modeling across the section somewhat obscures the geometry. Nonetheless, we feel it does explain many of the features observed in the seismic record. Fig. 8a thru 8d model a break-forward imbricate Devonian fold-and-thrust belt that developed first, with potentially significant topography. Fig. 8e and f model a thrust that was reactivated in negative inversion during the Carboniferous, but along a fault with both steepening and flattening segments. The convex bend across the steepening segment was due to the previously folded, contractional, second imbricate fault, and the concave bend was due to the normal fault taking advantage of the older contractional detachment horizon. Thus, the normal fault closely mimicked the contractional geometry of the westernmost thrust, resulting in the strange locally thick Ellesmerian section and related synclinal geometry of extensional growth strata. This stands in contrast with the previous example (Fig. 7), in which the normal fault cut across the older detachment. Local reactivation of the older contractional detachment suggests that here, in the center of the Hanna Trough during Carboniferous rifting, the older thrust-fault detachment

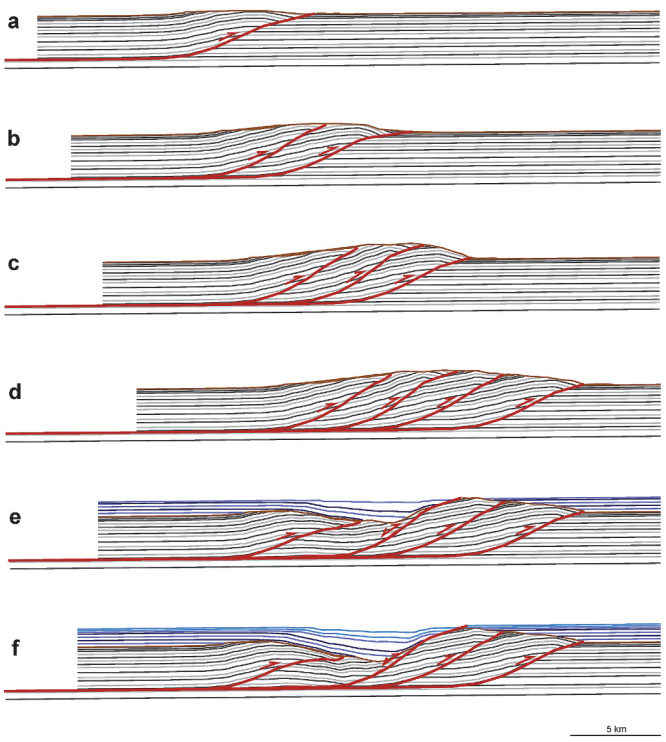

Fig. 8. Balanced sequential forward model of the negative inversion structure shown in the inset box of Fig. 5d a) through d) a break-forward imbricate Devonian fold-and-thrust belt develops and is eroded, causing the steep dip to the F2 section, and an angular truncation at the PMU. e) and f) Carboniferous extension reactivates one of the thrust planes in negative inversion where the normal fault reactivates a complex, older imbricate thrust geometry that changes from shallow to steeper and back to shallow with depth.

likely was weaker than the F1 strata in the footwall below the detachment. It is not known why that would be the case. We speculate it may be due to local facies changes, or fluid pressure along the detachment, or that the mid-crust in this locality lacks pre-F1 faults or weak zones. There is likely another reactivation in this complex structure, a component of Cenozoic extension, as discussed in a later section.

6. Late Jurassic-Early Cretaceous positive inversion

An interval of relative tectonic quiescence persisted from the Mississippian through the Triassic across Arctic Alaska during which the Hanna Trough evolved into a sag basin and the Chukchi and Arctic Platforms remained structural highs (Sherwood et al., 2002; Homza and Bergman, 2019). The upper part of the Ellesmerian megasequence strata reflect this quiescence, with generally carbonate and fine-grained siliciclastic deposition, including a relatively high proportion of petroleum source rocks in the Hanna Trough sag basin (Sherwood et al., 2002). The Lower and Middle Jurassic strata of the Beaufortian megasequence, including the lower part of the Kingak Shale, were likely deposited during this pausing of tectonism.

Tectonic activity was renewed in the Late Jurassic, with the initiation of rifting and opening of the North Chukchi and Canada Basins to the north and northeast, respectively (Grantz et al., 2011; Shephard et al., 2013; Hutchinson et al., 2017). To the south and southeast, closure of the South Anuyi ocean basin culminated in the Chukotka orogen and closure of the Angayucham ocean basin culminated in the Brooks Range orogen, respectively, during the Late Jurassic to Early Cretaceous (Shephard et al., 2013; Amato et al., 2015; Moore and Box, 2016). The Jurassic rifting events to the north impacted the Chukchi shelf by thermal bulging, rifting, and volcanism in parts of the Hanna Trough (Homza and Bergman, 2019). Strike-slip and contractional deformation of the North Chukchi high and "Grantz transpression zone" probably was under way during the Early Cretaceous (Neocomian) (Fig. 1; Homza and Bergman, 2019), although the age of initiation is not apparent. The closure of ocean basins to the south likely impacted at least the southern Chukchi shelf as fold-and-thrust belts associated with the Chukotka and Brooks Range orogens propagated northward, although the northern extent of Jurassic thrusting was located considerably south of the Wrangel-Herald Arch and current Brooks Range frontal fold-thrust belt shown in Fig. 1 (Moore and Box, 2016).

Beaufortian strata in the Chukchi shelf were significantly influenced by Jurassic to Early Cretaceous (Neocomian) deformation. In the northern Chukchi shelf and adjacent North Slope, a series of southward off-lapping sequence sets was deposited in response to rift-shoulder uplift associated with opening of the Canada Basin, constructing a series of west-northwest-oriented shelf margins (Hubbard et al., 1987; Sherwood et al., 2002; Houseknecht and Bird, 2004; Houseknecht and Connors, 2015; Homza and Bergman, 2019; Houseknecht, 2019a). However, across much of the Chukchi shelf, Beaufortian strata display eastward clinoform dip and north-oriented shelf margins; this has been interpreted as evidence for positive inversion of Carboniferous rift-phase normal faults (Houseknecht and Connors, 2015), as shown below.

Along the southern boundary between the Chukchi Platform and Hanna Trough, several north-trending, rift-phase normal faults display geometries that suggest they were inverted during Jurassic to Early Cretaceous (Fig. 6b). For example, in the structure shown in Fig. 9 (offset 87–90 km), growth strata of the lower part of the Ellesmerian thicken in the hanging wall, consistent with a normal sense of motion during Carboniferous faulting. Yet the top of the lower part of the Ellesmerian megasequence (PU) and the Jurassic unconformity (JU) are structurally higher on the hanging wall than on the footwall by about 0.5 s TWTT (close to 1 km), indicating subsequent reverse motion at depth on the fault. Moreover, the upper part of the Ellesmerian (PU to JU) conserves layer thickness, suggesting an intermediate time in which no motion on the fault occurred. Beaufortian strata expand across the front of the structure, and the Lower Cretaceous unconformity is structurally higher on the hanging wall than on the footwall, although the structural relief is less than on the Jurassic unconformity. These observations indicate accommodation was created during this time, with likely growth strata, and constrain the age of inversion to Jurassic to Early Cretaceous.

The details of the broader structure are less definitive; for example, a back limb to the structure is not clearly apparent locally. Thus, the structure does not fit the geometry of a classic positive inversion structure as defined by Williams et al. (1989). There are poor reflectors potentially associated with strata of the lower part of the Ellesmerian megasequence on the west side of the line in Fig. 9. Therefore, the structure could be characterized as a basement uplift with a frontal monocline, much like those in the Colorado Plateau (Bump, 2003). Because the upper part of the Ellesmerian section broadly conserves layer thickness in the east limb, and reactivated slip on the older fault is small, the fault-related folding kinematics of the front limb are ambiguous. The structural style in the front limb may involve low propagation-to-slip, trishear kinematics (Allmendinger, 1998), or it may be associated with contractional fault-bend-fold kinematics along a fault flattening to an upper detachment, with minor slip on the detachment dissipated into the center of the basin.

7. Complex Late Cretaceous-Paleogene contraction and positive inversion

Cretaceous and Paleogene tectonics in the Chukchi shelf region mainly involved development of the fold-and-thrust belts of the Wrangel-Herald Arch (frontal belt of Chukotka orogen) and western Brooks Range. These events included significant uplift and exhumation, which shed a huge volume of siliciclastic sediment into the foreland, as well as contractional deformation of the western Colville foreland basin in the southern Chukchi shelf and adjacent North Slope (Mull et al.,

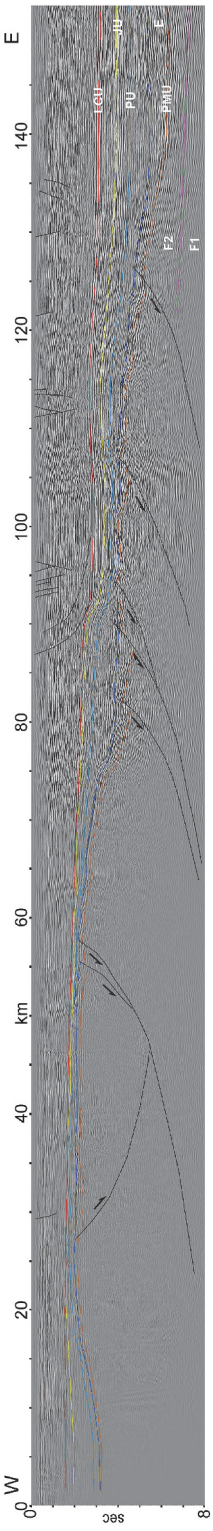

Fig. 9. Seismic line from the southern Hanna Trough. See Fig. 1 for location. Shown with approximately no vertical exaggeration for the deeper reflective section. Mississippian crustal extension is inverted in the Late Jurassic to Early Cretaceous in a contractional event forming a asymmetric positive inversion structure. Franklinian, lower part (F1); Franklinian, upper part (F2); pre-Mississippian unconformity (PMU); Endicott Group equivalent (E); Permian unconformity (PU); Jurassic unconformity (JU); Lower Cretaceous unconformity (LCU).

2000; Moore et al., 2002; Sherwood et al., 2002; Moore et al., 2015; Moore and Box, 2016; Craddock and Houseknecht, 2016; Craddock et al., 2018; Homza and Bergman, 2019; Houseknecht, 2019b; Lease et al., 2022, Fig. 1). However, the thin-skinned folding and thrusting in this foreland position are locally detached at or near the Lower Cretaceous unconformity and thus no structural inheritance or inversion is apparent.

In contrast, Cretaceous to possibly Paleogene contraction in the northern Chukchi shelf is expressed in a different structural style, including complex interactions with older structures. The North Chukchi high (Thurston and Theiss, 1987; Johnson, 1990; Sherwood et al., 2002; Homza and Bergman, 2019, Figs. 3 and 6c), a basement uplift with substantial structural relief between the base of the Hanna Trough on the south to the crest of the structural high (Fig. 10), is the most distinctive expression of this deformation. The Hanna Trough, shown in the south part of Fig. 10, displays regional unconformities that show a reflective character similar to seismic images previously shown, with approximately consistent megasequence thicknesses in this orientation. In the center of the line (offset 45–80 km) a strong series of reflectors cannot be correlated below ~1 s TWTT and deeper data show substantial conflicting energy. Based on regional ties and the reflective character in this image, including local swings in reflectivity, we interpret that these likely are seismic artifacts in an otherwise reflective-poor, seismically quiescent, Franklinian section. The north part of the line (offset 85–100 km) shows improved reflective character that can be mapped beneath, as well as truncating against, the seismically quiescent section. We tentatively interpret a PMU extending northward, but more work is warranted to better constrain the age of the section below this prominent unconformity. The LCU and KPU can be tied regionally, constraining the age of the younger strata and deformation.

We interpret the structural relief (more than 10 km) across the southern boundary of the North Chukchi high to be the result of large, south-vergent, contractional fault-bend folds along north-dipping imbricate thrusts (Fig. 10). Parallel folding just south of the high (offset 20–35 km) suggests contractional deformation by flexural slip and southward tectonic transport is constrained by the major structural relief through imbrication that brought the top of the pre-Mississippian section close to the seafloor in places. Fold limbs comprising Upper Cretaceous strata in angular truncation by the KPU brackets the timing of latest contraction to Late Cretaceous-early Paleogene. The southward tectonic transport from causative deep thrusts that step up to a local detachment in the lower part of the Ellesmerian section in the center of the Hanna Trough significantly constrains the interpretation. No additional contractional structures that can be linked to this detachment have been observed to the south in the Hanna Trough and, therefore, slip must be transferred back to the north as structural wedges in a triangle zone. Just north of this triangle zone (offset 40–55 km), south-directed thrust imbrication bring Franklinian basement close to the seafloor, providing some of the observed structural relief across the southern boundary of the North Chukchi high. The wedge interpretation requires some late south-directed thrusting to cut the roof thrust, but there may have been a component of earlier thrusting on these faults and associated uplift.

We interpret the northern boundary of the North Chukchi high to be bounded by deep-seated, south-dipping thrust faults that ramped northward up to a Cretaceous paleo-seafloor, forming local fault-bend folds. This likely occurred in the absence of significant local sediment cover at the time of thrusting, as constrained by the lack of folded growth strata in the lower Brookian megasequence. We interpret shortening to have commenced in the Aptian, as constrained by folding of the LCU and overlying Lower Cretaceous strata, and truncation by the KPU (offset 85–90 km in Fig. 10). Such deformation would be approximately coeval with deposition of the "Kalubik wedge," a lower Brookian succession unique to the Chukchi shelf that shed southward from the North Chukchi high (Homza and Bergman, 2019). These observations imply that uplift across the southern boundary of the high also occurred

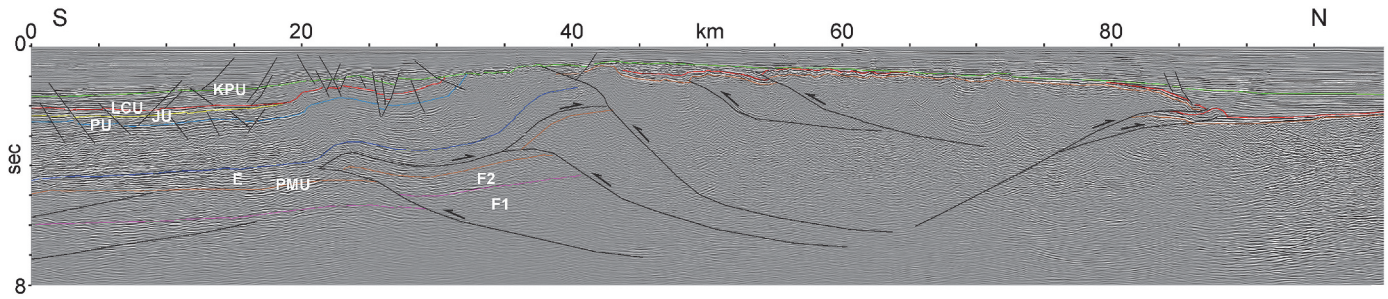

Fig. 10. North-south seismic line straddling the northeast side of Hanna Trough and south side of the North Chukchi high. See Fig. 1 for location. Shown with approximately no vertical exaggeration for the deeper reflective section. The North Chukchi high is a north- and south-directed, contractional imbricate system involving much of the upper crust. On the northeast side of the Hanna Trough Mississippian crustal extension is inverted in a Late Cretaceous-early Paleogene positive inversion contractional event at a high angle to older structures. Franklinian, lower part (F1); Franklinian, upper part (F2); pre-Mississippian unconformity (PMU); Endicott Group equivalent (E); Permian unconformity (PU); Jurassic unconformity (JU); Lower Cretaceous unconformity (LCU); Cretaceous-Paleogene unconformity (KPU).

at this time, but direct evidence of that timing apparently was obliterated by later thrusting, as discussed above.

Overall structural relief across the North Chukchi high suggests thrusts root in a mid-crustal detachment, likely as a distributed shear zone with associated crustal thickening, given the inferred depth at the time of deformation. The depth of the inferred detachment is similar to that of the Carboniferous rift-related detachment just to the south (Fig. 11). We speculate that the rift-related detachment may have localized the later contractional detachment, although it is difficult to demonstrate the extent of structural inheritance because the contractional inversion is nearly orthogonal to the older normal faults. Sherwood et al. (2002) proposed that the southern boundary of the North Chukchi high was an inverted Carboniferous transform fault that offset the Hanna Trough rift segment from an inferred rift segment in the North Chukchi Basin to the west. If that is the case, then this would indeed constitute true structural inheritance, at a basin-scale.

Homza and Bergman (2019) document this trend of Late Cretaceous to Paleogene contraction also near the Popcorn well (Fig. 6c) which they termed the Popcorn high. We concur with this interpretation and propose that this is a continuation of a ~300-km-long regional contractional belt (Fig. 6c), obscured by later Cenozoic deformation. Given the multiple phases of growth to the structures, and the proximity to older Carboniferous rifts, the Popcorn high is another form of structural inheritance whereby the older Carboniferous north-south striking, rift-related normal faults act as strike-slip faults in the Cretaceous to Paleogene. These tear faults bound the southward-transported contractional structures (Fig. 6c). In this scenario the Popcorn high is both a Carboniferous horst, and a later Cretaceous to Paleogene block of imbricate thrusts. The east-west orientation of the line in Fig. 11b thus captures the dip-slip component to Carboniferous extension, whereas the north-south Cretaceous to Paleogene shortening occurs as motion in and out of the plane of the section. Subsequent Cenozoic extension resulted in another structural reactivation, as discussed in the subsequent section.

Late Cretaceous-early Paleogene structural inheritance in the Hanna Trough is also manifest just southeast of the main North Chukchi high (Fig. 11c). Timing of contraction is constrained by the folded LCU and Lower Cretaceous strata (offset 230 km), similar to the nearby North Chukchi high (Fig. 10). Superficially, the structure in Fig. 11c looks like a positive inversion structure (Williams et al., 1989) associated with reactivation of a Carboniferous normal fault, with a long back limb and short front limb, a normal sense of motion at depth, and positive relief in the shallow horizons. However, this and other similar structures in the area likely were reactivated in oblique positive inversion. These structures strike in a discontinuous approximately north-south direction (Fig. 6c). If some displacement associated with the North Chukchi high was sent southward along a mid-crustal detachment and encountered Carboniferous normal fault geometries that strike north-south, then highly oblique structures associated with lateral boundaries of this enigmatic Late Cretaceous-Paleogene contractional event are plausible.

8. Cenozoic extensional reactivation of rift features

Cenozoic strata in the Chukchi shelf represent a continuation of Brookian megasequence sedimentation associated with northward routing of sediments derived from Chukotka and the western Brooks Range (Thurston and Theiss, 1987; Sherwood et al., 2002; Houseknecht and Bird, 2011; Homza and Bergman, 2019). Most of these previous authors invoke transtensional and transpressional deformation in the Chukchi shelf in the Cenozoic based on interpreted flower structures on vertically exaggerated seismic sections. While some strike-slip component is likely present, it is challenging to ascertain this from a regional 2D seismic grid. When seismic lines in the area are examined with approximately no vertical exaggeration, it is clear that extension is ubiquitous, with a significant inheritance from previous structures.

Inspection of seismic data from the northern Chukchi Platform shows clear reflectors in the top 3 s TWTT that can be followed across discrete high-angle boundaries, with reflector offset, and in places dip into the boundaries (Fig. 11). These reflector geometries and correlation of regional unconformities indicate fault reactivation during Cenozoic crustal extension along mainly east-dipping, normal faults that are high-angle near the surface and sole to a mid-crustal detachment (Fig. 11a). Ellesmerian growth strata in the eastern grabens indicate Early Mississippian extension. Paleocene to Pliocene structural reactivation is evident by offset of the KPU and post-Paleogene growth strata (Fig. 11a). Ellesmerian strata thin to the west, but the relationship of older faults being reactivated discretely in the Cenozoic holds. On the east side of the line (Fig. 11a, offset 80–85 km), salt deposition in the Carboniferous, with modest reactive diapirism in the Cenozoic (Thurston and Lothamer, 1991; Homza and Bergman, 2019), is consistent with these two phases of crustal extension.

In contrast, in the central Hanna Trough, despite the fact that discrete Carboniferous rift-related normal faults mainly dip west, Cenozoic faults dip in both directions, in a more distributed fashion, forming local half grabens (Fig. 11b). In many cases, the seismic imaging is insufficient to resolve the fault geometry at depth, which may suggest these Cenozoic faults sole in a complex fashion into a local detachment in the upper part of the Ellesmerian, or alternatively strain may be distributed below seismic resolution at this stratigraphic interval. The strikes of minor Cenozoic normal faults are difficult to determine because of the modest throw and regional seismic grid spacing. Nonetheless, if the sections are displayed with little vertical exaggeration one can infer a nominally true dip orientation of east and west because these Cenozoic faults are high-angle and thus approximate the primary fault geometry shown in Fig. 11b. Thus, this Cenozoic extension is mostly east-west, mimicking the earlier extension direction.

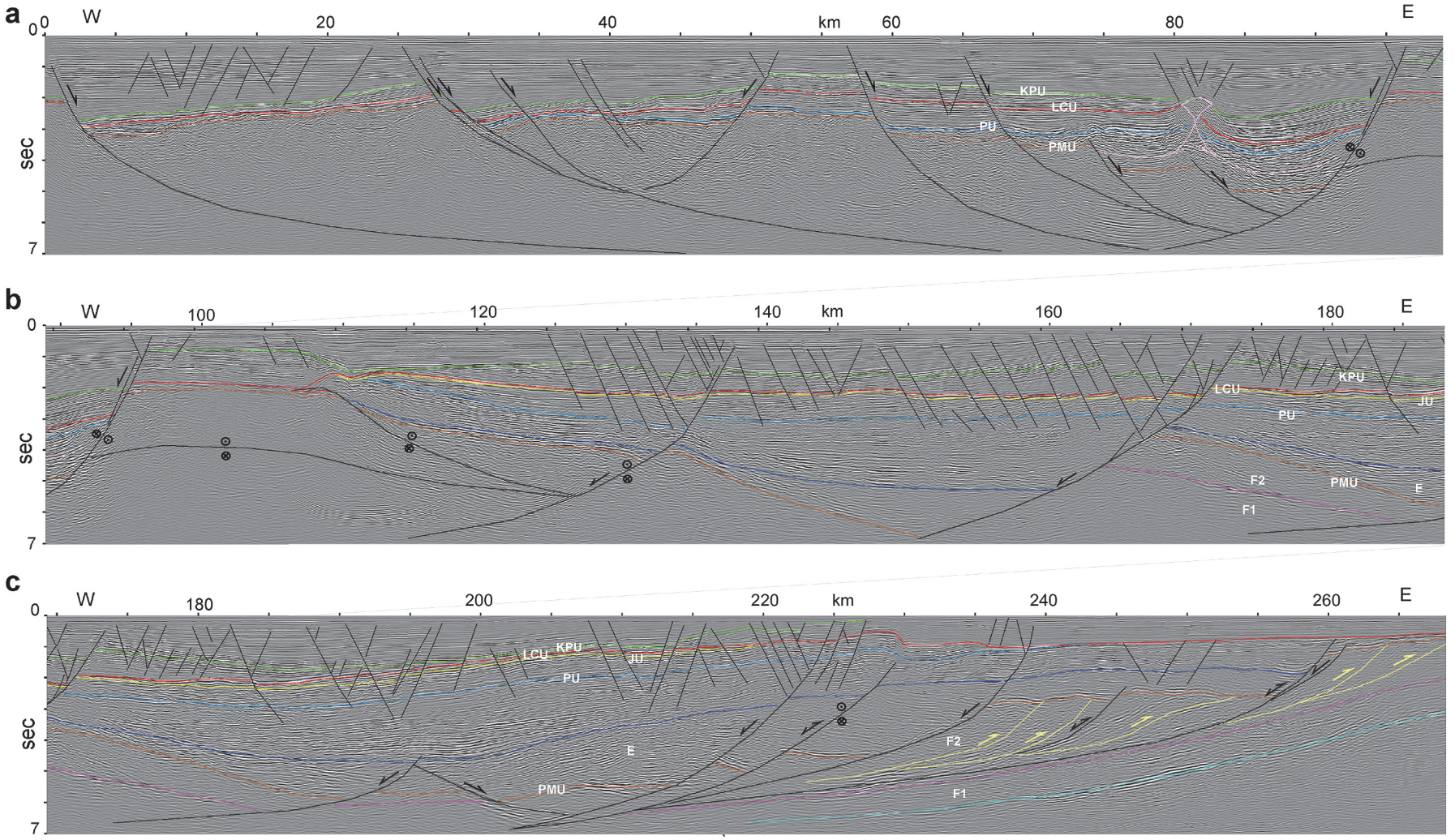

Fig. 11. Enlargement of the seismic line shown in Fig. 4. See Fig. 1 for location. Shown with approximately no vertical exaggeration for the deeper reflective section. Franklinian, lower part (F1); Franklinian, upper part (F2); pre-Mississippian unconformity (PMU); Endicott Group equivalent (E); Permian unconformity (PU); Jurassic unconformity (JU); Lower Cretaceous unconformity (LCU); Cretaceous-Paleogene unconformity (KPU). Each segment of the line shows varying influence of Mississippian crustal normal faults on later deformation. a) Mississippian crustal normal faults in the Chukchi Platform (west side of line segment) and northwestern Hanna Trough are discretely reactivated in a second extension during the Neogene. On the eastern side of the segment, Neogene reactive salt diapirism is present locally. b) Continuation of line segment in (a) Late Cretaceous-early Paleogene south-directed, imbricate thrusting (motion in and out the plane of section) deforms the older horst. Mississippian crustal normal faults locally reactivate in strike slip. Subsequently Mississippian crustal normal faults in the northern Hanna Trough are reactivated in a distributed fashion, coalescing at depth during a second extension during the Neogene. c) Continuation of line segment (b) showing multiple tectonic events superimposed. These include Devonian thin-skinned fold-and-thrust belt, reactivated in negative inversion during Carboniferous crustal extension. This is followed by Late Cretaceous, oblique, positive inversion (with some motion out of the plane of section), and finally with Cenozoic extensional reactivation.

Supporting this is the fact that there is an increased amount of Cenozoic extension above the older rifts, and thus these Cenozoic faults appear related to the older extensional fabric, as is interpreted on the fault in the center of the section in Fig. 11b (offset 165–175 km). This suggests that a local response to renewed crustal rifting occurred in places. A similar localized Cenozoic extensional reactivation is observed above the Carboniferous negative inversion structure shown in Fig. 5d. Cenozoic normal faults also cut the Late Cretaceous inversion structures discussed in the previous section, but not necessarily at original, Carboniferous rifts. An example is observed in the Cenozoic faults on the crest and back limb of the inversion structure in Fig. 11c (offset 220–225 km). The contrast between distributed Cenozoic extension in the Hanna Trough, and discrete Cenozoic extension in the Chukchi Platform may be due to local variations in mechanical strength in the lithosphere related to the amount of post-rift section in each area.

9. Discussion

9.1. Tectonic implications

Several observations presented here are consistent with the Chukchi Platform being the hinterland, and the Arctic Platform the foreland, of a major middle Paleozoic convergent margin. These include: 1) the change in seismic character of the F2 (likely Upper Ordovician-Devonian) section across the Hanna Trough, 2) the fold vergence and tectonic transport to the east, and 3) the detached style in the Arctic Platform. Sherwood et al. (2002) proposed that the high magnetic signature in the Chukchi Platform may reflect volcanic arc rocks juxtaposed against sedimentary strata to the east in the Hanna Trough and Arctic Platform. Miller et al. (2017) proposed that the Chukchi Platform is the metamorphic core of the Arctic Caledonian orogen related to the suturing of Pearya onto Laurentia. This would be a southern extension of the Pearya-Laurentia terrane boundary in the Chukchi borderland proposed by O'Brien et al. (2016) based on dredge samples and consistent with earlier dredge and core samples from Grantz et al. (1998). Homza and Bergman (2019) likewise postulated a suture between Pearya and Laurentia along the Hanna Trough. On the eastern flank of the Hanna Trough and western margin of the Arctic Platform thick-skinned contraction involving much of the Franklinian megasequence has been proposed (Kumar et al., 2011). Miller et al. (2017) interpreted this to be the basement-involved thrust front of the Arctic Caledonian orogen. As discussed above, we interpret the F1 to not be involved in contraction, and instead have a detached fold-and-thrust belt lying above it. Thus, this contraction may be a thin-skinned foreland of the final vestiges of the Arctic Caledonian orogen, in the Late Silurian to Early Devonian. Similar aged contractional structures and uplift have been observed in the Canadian Arctic Islands related to the Boothia event (Harrison, 2018; Dewing et al., 2019). Alternatively, the deformation may be analogous with the Early to Middle Devonian Romanzof orogeny in northwestern Yukon and Arctic Alaska (Lane, 2007). The folding and thrusting could also potentially be Late Devonian to Early Mississippian, similar to the Ellesmerian orogeny of Arctic Canada (Trettin et al., 1991; Embry, 1991; Harrison and Brent, 2005; Beranek et al., 2010). In short, at this point timing of the fold-and-thrust belt involving the F2 strata is poorly constrained because timing of the section itself is not well known.

At a basin-scale, crustal normal faults that cut the pre-Mississippian unconformity (PMU) are present in much of the same area as the observed pre-Mississippian (likely Devonian) fold-and-thrust belt (compare Fig. 5a and b). These rifts also extend west beyond the main Hanna Trough and into the Chukchi Platform (Figs. 4 and 6b). The close correspondence in space and time of contraction followed by extension, as well as the fault-fold geometries discussed previously, suggest post-orogenic collapse (Dewey, 1988) in the hinterland of the older fold-and-thrust belt to form the Hanna Trough, consistent with the views of Homza and Bergman (2019).

The Late Jurassic-Early Cretaceous positive inversion of Carboniferous rift-related normal faults resulted in localized west-east shortening (Fig. 6b). The fact that they are localized in the southern Hanna Trough (Fig. 6b) suggests they may be a far-field effect of oblique contraction in the foreland of the Chukotkan orogeny (Houseknecht and Connors, 2015; Homza and Bergman, 2019).

The North Chukchi high represents a significant regional, if poorly understood, contractional feature in the Arctic. Formation of it overlaps temporally with contractional deformation in the Wrangel-Herald Arch and western Brooks Range but lies about 200 km north of the foreland structures (Fig. 1) and nearly 400 km north of the main orogens (Moore and Box, 2016). Homza and Bergman (2019) pointed out the connection to the east-northeast trending "Grantz transpressional zone" (Fig. 1), although the extent and kinematic role of a transverse component in forming the north- and south-vergent contractional structures remain unknown.

The greatest Cenozoic extension is in the northern Hanna Trough and diminishes to the south (Fig. 6c). Unmapped at this time is the complex Cenozoic extension at the margin of the North Chukchi Basin. Related extension may link to the Chukchi borderland (Fig. 1), where existing fault scarps are pronounced in bathymetry (Ilhan and Coakley, 2018). This extension at the margin of the North Chukchi Basin speculatively may be due more to far-field, plate-related mechanisms, perhaps related to opening of the Eurasia Basin and northward propagation of the Mid-Atlantic Ridge in the Cenozoic (Shephard et al., 2013).

9.2. Petroleum systems implications

Petroleum systems elements of the Chukchi shelf are summarized below, based on Sherwood et al. (1998, 2002), Houseknecht et al. (2012), Villegas et al. (2017), Homza and Bergman (2019), and Houseknecht (2021, 2022). Known and potential oil-prone source rocks are concentrated in and near the Hanna Trough, particularly in Carboniferous to Lower Jurassic sag-basin deposits. Known source rocks are present in the Triassic Shublik Formation, distal facies of the Triassic Sadlerochit Group, and Jurassic Kingak Shale. Potential source rocks may occur in the Carboniferous Lisburne Group (Fig. 2). Source rocks also are known in Cretaceous foreland basin deposits of the informally named pebble shale unit (PSU) and gamma-ray zone (GRZ), although these tend to be of lower quality than coeval strata in the North Slope and Beaufort shelf. Source rocks are postulated to occur in Cenozoic strata in the northern Chukchi shelf, most likely in distal facies of Barremian to Turonian and Eocene strata. Known and potential reservoir rocks occur throughout the Phanerozoic stratigraphic section, mainly in sandstone but also in carbonate rocks of the Lisburne Group. Two- and three-dimensional seismic data reveal a spectrum of stratigraphic, structural, and combination trap geometries spanning the stratigraphic column and present across much of the Chukchi shelf. Seals are mainly shale throughout the region and evaporite seals may be present locally in grabens known to contain evaporites within the Ellesmerian megasequence, mainly in the northwestern Chukchi shelf.

Burial history modeling suggests that oil generation from pre-Cretaceous source rocks occurred during the Early to Late Cretaceous and from Cretaceous and Cenozoic source rocks during the Late Cretaceous to Neogene. Within this temporal context, structural inheritance may have exerted both positive and negative influences on the occurrence and preservation of hydrocarbon accumulations. Early Cretaceous and older structural events likely had little influence on petroleum systems other than creating potential migration pathways and traps for hydrocarbons generated during subsequent burial. However, Late Cretaceous and younger structural events may have influenced petroleum systems elements significantly.

Late Cretaceous to Paleogene contraction and positive inversion likely post-dated or temporally overlapped hydrocarbon generation in Lower Cretaceous and older source rocks. The most likely positive influence may have been the creation of potential migration pathways and structural and combination traps that may have formed during or

shortly following hydrocarbon generation; natural gas trapped in the Burger anticline may be an example. Negative influences may have included uplift and exhumation of strata comprising potential carrier beds and reservoir rocks, resulting in migration to the ground surface or seafloor; the non-productive Popcorn anticline may be an example.

Cenozoic extensional reactivation of rift features likely post-dated or temporally overlapped hydrocarbon generation in Lower Cretaceous source rocks. Positive results may have included creation of diapiric traps (salt domes) and seals in evaporite-bearing grabens and formation of structural traps comprising rotated fault blocks and other transpressional closures; none of these trap types has been tested. Negative results may have included fracture-breaching of older traps and seals leading to remigration of previously trapped hydrocarbons to the ground surface or sea floor.

10. Conclusion and future work

We have presented several seismic examples of structural inheritance in the Chukchi shelf, Alaska. These include: 1) Carboniferous negative inversion of a Devonian east-vergent fold-and-thrust belt widespread within the Hanna Trough and Arctic Platform, 2) Late Jurassic-Early Cretaceous positive inversion of Carboniferous rift-related normal faults, 3) Late Cretaceous-Paleogene positive inversion in the North Chukchi High, and 4) Cenozoic extension and strike-slip reactivation and negative inversion manifest in a variety of forms in the northern Chukchi shelf. The multiple episodes of reactivation show that structural inheritance can be passed down through multiple generations during the tectonic evolution of an area. The fact that such structures are spatially so close shows how important it is to consider inheritance in an interpretation.

The North Chukchi high, particularly its northern boundary, is not well constrained and merits further study. Determining the lateral extent of reactivation and more complete 3D geometry of the North Chukchi high polyphase deformation is a logical next step. Because of the extent of structural inheritance, and changing tectonic transport directions over time, 3D modeling and balancing or restoration based on interpretations from depth-migrated images may be required, and would lend additional confidence in, or modifications to, the interpretations presented here. Such work would require unraveling the Cenozoic extension and strike-slip faulting in the area, in and of itself poorly understood. Mapping out in more detail the nature of Cenozoic extension as it extends into the poorly known North Chukchi Basin and Chukchi borderland would likewise be useful, and has implications for circum-Arctic Cenozoic tectonics.

Credit author statement

Connors: Conceptualization, Methodology, Formal analysis, Investigation, Data Curation, Writing - Original Draft, Writing - Review & Editing, Visualization, Funding acquisition. **Houseknecht:** Investigation, Writing - Original Draft, Writing - Review & Editing, Visualization.

Declaration of competing interest

The authors declare that they have no known competing financial interests or personal relationships that could have appeared to influence the work reported in this paper.

Data availability

The data that has been used is confidential.

Acknowledgements

We are delighted to contribute to the volume in honor of Bert Bally. He was a pioneer in so many areas of structural geology, including aspects that are touched on in this work: structural interpretation of seismic data, structural inversion, and regional tectonics. The manuscript has been greatly improved by the comments of Joan Flinch, Tom Homza, Ben Johnson, Piotr Krzywiec, and Scott Young. Several Washington and Lee undergraduate research students participated in early aspects of the interpretations of the Chukchi shelf presented here, and we would like to recognize discussions with Charlie Gentry, Andy Roberts, Arthur Stier, Andrew Clements, Blake Odom, and Harris Pritchard. Connors is grateful for the generous support from the Lenfest and Young Funds at Washington and Lee University. The first author also acknowledges IHS Markit for permission to use the software Kingdom Suite through the University Grant Program. We are grateful for permission, by a company that wishes to remain anonymous, for the seismic data shown. This work was supported by the National Science Foundation [grant number EAR1946680].

References

Allmendinger, R.W., 1998. Inverse and forward numerical modeling of trishear fault-propagation folds. Tectonics 17, 640–656.
Amato, J.M., Toro, J., Akinin, V.V., Hampton, B.A., Salnikov, A.S., Tuchkova, M.I., 2015. Tectonic evolution of the Mesozoic South Anyui suture zone, eastern Russia: a critical component of paleogeographic reconstructions of the Arctic region. Geosphere 11, 1530–1564. https://doi.org/10.1130/GES01165.1.
Bally, A.W., 1984. Tectogenèse et sismique réflexion. Bull. Soc. Geol. Fr. 7, 279–285.
Bally, A.W., Gordy, P.L., Stewart, G.A., 1966. Structure, seismic data, and orogenic evolution of Southern Canadian Rocky Mountains. Bull. Can. Petrol. Geol. 14, 337–381.
Beranek, L., Mortensen, J., Lane, L., Allen, T., Fraser, T., Hadlari, T., Zantvoort, W., 2010. Detrital zircon geochronology of the western Ellesmerian clastic wedge northwestern Canada: insights on Arctic tectonics and the evolution of the northern Cordilleran miogeocline. Geol. Soc. Am. Bull. 122, 1899–1911. https://doi.org/10.1130/B30120.1.
Bird, K.J., 2001. Alaska: a twenty-first-century petroleum province. In: Downey, M.W., Threet, J.C., Morgan, W.A. (Eds.), Petroleum Provinces of the Twenty-First Century, vol. 74. American Association of Petroleum Geologists, Tulsa, OK, Memoirs, pp. 137–165.
Buchanan, J.G., Buchanan, P.G. (Eds.), 1995. Basin Inversion, vol. 88. Geological Society of London, p. 596. Special Publications.
Bump, A.P., 2003. Reactivation, trishear modeling, and folded basement in Laramide uplifts: implications for the origins of intra-continental faults. GSA Today (Geol. Soc. Am.) 13, 4–10.
Byerlee, J.D., 1978. Friction of rocks. Pure Appl. Geophys. 116, 615–626.
Carter, C., Laufeld, S., 1975. Ordovician and Silurian fossils in well cores from the North Slope of Alaska. AAPG (Am. Assoc. Pet. Geol.) Bull. 103, 619–652.
Connors, C.D., Hughes, A.N., Ball, S.M., 2021. Kinematic forward modeling of fault-bend folding. J. Struct. Geol. 143, 1–21. https://doi.org/10.1016/j.jsg.2020.104252.
Constenius, K.N., 1996. Late Paleogene extensional collapse of the Cordilleran foreland fold and thrust belt. Geol. Soc. Am. Bull. 108, 20–39.
Cooper, M.A., Williams, G.D. (Eds.), 1989. Inversion Tectonics, vol. 44. Geological Society of London, Special Publications, p. 375.
Craddock, W.H., Houseknecht, D.W., 2016. Cretaceous-Cenozoic burial and exhumation history of the Chukchi shelf, offshore Arctic Alaska. AAPG (Am. Assoc. Pet. Geol.) Bull. 100, 63–100. https://doi.org/10.1306/09291515010.
Craddock, W.H., Moore, T.E., O'Sullivan, P., Potter, C.J., Houseknecht, D.W., 2018. Late Cretaceous–Cenozoic exhumation of the western Brooks Range, Alaska, revealed from apatite and zircon fission track data. Tectonics 37, 414–4751. https://doi.org/10.1029/2018TC005282.
Craig, J.D., Sherwood, K.W., Johnson, P.P., 1985. Geologic Report for the Beaufort Sea Planning Area, Alaska. US Minerals Management Service, p. 192. OCS Report MMS 85–0111.
Dewey, J.F., 1988. Extensional collapse of orogens. Tectonics 7, 1123–1139.
Dewing, K., Hadlari, T., Pearson, D.G., Mathews, W., 2019. Early Ordovician to Early Devonian tectonic development of the northern margin of Laurentia, Canadian Arctic Islands. Geol. Soc. Am. Bull. 131, 1075–1094.
Dumoulin, J.A., 2001. Lithologies of the basement complex (Devonian and older) in the national petroleum reserve–Alaska. In: Houseknecht, D.W. (Ed.), NPRA Core Workshop—Petroleum Plays and Systems in the National Petroleum Reserve—Alaska, Society for Sedimentary Geology, vol. 21. Core Workshops, Tulsa, OK, pp. 201–214.
Embry, A.F., 1990. Geological and geophysical evidence in support of the hypothesis of anticlockwise rotation of northern Alaska. Mar. Geol. 93, 317–329. https://doi.org/10.1016/0025-3227(90)90090-7.
Embry, A.F., 1991. Middle–Upper Devonian clastic wedge of the Arctic Islands. In: Trettin, H.P. (Ed.), Geology of the Innuitian Orogen and Arctic Platform of Canada and Greenland. Ottawa, Canada, vol. 3. Geological Survey of Canada, Geology of Canada, pp. 261–279.
Fox, F.G., 1985. Structural geology of the Parry Island fold belt. Bull. Can. Petrol. Geol. 33, 306–340.

Glennie, K.W., Boegner, P.L.E., 1981. Sole pit inversion tectonics. In: Illing, L.V., Boegner, P.L.E. (Eds.), Petroleum Geology of the Continental shelf of NW Europe. Institute of Petroleum London, pp. 110–120.
Grantz, A., Dinter, D.A., Hill, E.R., Hunter, R.E., May, S.D., McMullin, R.H., Phillips, R.L., 1982. Geologic framework, hydrocarbon potential, and environmental conditions for exploration and development of proposed oil and gas lease sale 87 in the Beaufort and Northeast Chukchi Seas: U.S. Geological Survey Open File Report 82–482, 72.
Grantz, A., May, S.D., Hart, P.E., 1994. Geology of the Arctic continental margin of Alaska. In: Plafker, G., Berg, H.C. (Eds.), The Geology of Alaska. Geological Society of America, The Geology of North America, G-1, pp. 17–48.
Grantz, A., Clark, D.L., Phillips, R.L., Srivastava, S.P., 1998. Phanerozoic stratigraphy of Northwind ridge, magnetic anomalies in the Canada Basin, and the geometry and timing of rifting in the Amerasia Basin, Arctic Ocean. Geol. Soc. Am. Bull. 110, 801–820.
Hadlari, T., Davis, W.J., Dewing, K., 2014. A pericratonic model for the Pearya terrane as an extension of the Franklinian margin of Laurentia, Canadian Arctic. Geol. Soc. Am. Bull. 126, 182–200. https://doi.org/10.1130/B30843.1.
Handy, M.R., 1989. Deformation regimes and the rheological evolution of fault zones in the lithosphere: the effects of pressure, temperature, grainsize and time. Tectonophysics 163, 119–152.
Hansen, W.R., 1986. Neogene Tectonics and Geomorphology of the Eastern Uinta Mountains in Utah, Colorado, and Wyoming, vol. 1356. U. S. Geological Survey Professional Paper, p. 78.
Harrison, J.C., 2018. Intersecting fold belts in the Bathurst Island region, nunavut. J. Geodyn. 118, 82–105.
Harrison, J.C., Bally, A.W., 1998. Cross-sections of the Parry Islands fold belt on Melville Island, Canadian Arctic Islands: implications for the timing and kinematic history of some thin-skinned decollement systems. Bull. Can. Petrol. Geol. 36, 311–332.
Harrison, J.C., Brent, T.A., 2005. Basins and fold belts of Prince Patrick Island and adjacent areas Canadian Arctic Islands. Geol. Surv. Can. Bull. 560, 197. https://doi.org/10.4095/220345.
Holdsworth, R.E., Butler, C.A., Roberts, A.M., 1997. The recognition of reactivation during continental deformation. J. Geol. Soc. 154, 73–78. London.
Homza, T.X., Bergman, S.C., 2019. A Geologic Interpretation of the Chukchi Sea Petroleum Province, Offshore Alaska, USA, vol. 119. Association of Petroleum Geologists Memoirs, p. 330. https://doi.org/10.1306/AAPG119.
Houseknecht, D.W., 2019a. Evolution of the arctic Alaska sedimentary basin. In: Miall, A. D. (Ed.), The Sedimentary Basins of the United States and Canada. Elsevier, pp. 719–745. https://doi.org/10.1016/B978-0-444-63895-3.00018-8.
Houseknecht, D.W., 2019b. Petroleum systems framework of significant new oil discoveries in a giant Cretaceous (Aptian–Cenomanian) clinothem in Arctic Alaska. AAPG (Am. Assoc. Pet. Geol.) Bull. 103, 619–652. https://doi.org/10.1306/08151817281.
Houseknecht, D.W., 2021. Arctic Alaska Basin, Hanna trough, and Beaufortian rifted margin composite tectono-sedimentary elements. In: Drachev, S.S., Brekke, H., Henriksen, E., Moore, T.E. (Eds.), Sedimentary Successions of the Arctic Region and Their Hydrocarbon Prospectivity. Geological Society of London. Memoir 57.
Houseknecht, D.W., 2022. Colville foreland basin and Arctic Alaska prograded margin tectono-sedimentary elements. In: Drachev, S.S., Brekke, H., Henriksen, E., Moore, T. E. (Eds.), Sedimentary Successions of the Arctic Region and Their Hydrocarbon Prospectivity. Geological Society of London. Memoir 57.
Houseknecht, D.W., Bird, K.J., 2004. Sequence stratigraphy of the Kingak shale (Jurassic–Lower Cretaceous), National Petroleum Reserve in Alaska. AAPG (Am. Assoc. Pet. Geol.) Bull. 88, 279–302.
Houseknecht, D.W., Bird, K.J., 2011. Geology and petroleum potential of the rifted margins of the Canada Basin. In: Spencer, A.M., Embry, A.F., Gautier, D.L., Stoupakova, A.V., Sørensen, K. (Eds.), Arctic Petroleum Geology, vol. 35. Geological Society of London Memoir, pp. 509–526.
Houseknecht, D.W., Connors, C.D., 2015. Late Jurassic – Early Cretaceous inversion of rift structures, and linkage of petroleum system elements across post-rift unconformity, US Chukchi shelf, Arctic Alaska. In: Post, P.J., Coleman Jr., J.L., Rosen, N.C., Brown, D.E., Roberts-Ashby, T., Kahn, P., Rowan, M. (Eds.), Petroleum Systems in "Rift" Basins. Gulf Coast Section SEPM, 34th Annual Gulf Coast Section SEPM Foundation Perkins-Rosen Research Conference, Proceedings, p. 15.
Houseknecht, D.W., Connors, C.D., 2016. Pre-Mississippian tectonic affinity across the Canada Basin – Arctic margins of Alaska and Canada. Geology 44, 507–510. https://doi.org/10.1130/G37862.1.
Houseknecht, D.W., Burns, W.M., Bird, K.J., 2012. Thermal maturation history of Arctic Alaska and southern Canada Basin. In: Harris, N.B., Peters, K.E. (Eds.), Thermal History Analysis of Sedimentary Basins—Methods and Case Histories, vol. 103. Society for Sedimentary Geology, pp. 199–219. Special Publication.
Hubbard, R.J., Edrich, S.P., Rattey, R.P., 1987. Geologic evolution and hydrocarbon habitat of the 'Arctic Alaska microplate.'. Mar. Petrol. Geol. 4, 2–34.
Hutchinson, D.R., Jackson, H.R., Houseknecht, D.W., Li, Q., Shimeld, J.W., Mosher, D., Chian, D., Saltus, R.W., Oakey, G.N., 2017. Significance of northeast-trending features in the Canada Basin, Arctic Ocean. G-cubed 18, 4156–4178. https://doi.org/10.1002/2017GC007099.
Ilhan, I., Coakley, B.J., 2018. Meso–Cenozoic evolution of the southwestern Chukchi borderland, Arctic Ocean. Mar. Petrol. Geol. 95, 100–109. https://doi.org/10.1016/j.marpetgeo.2018.04.014.
Jackson, J.A., 1980. Reactivation of basement faults and crustal shortening in orogenic belts. Nature 283, 343–346.
Johnson, P.P., 1990. Multiple-stage deformation along the southern flank of the North Chukchi high, Chukchi Sea, Alaska. AAPG Annual Convention & Exhibition, San Francisco, Abstract.
Kumar, N., Granath, J.W., Emmet, P.A., Helwig, J.A., Dinkelman, M.G., 2011. Stratigraphic and tectonic framework of the US Chukchi shelf: exploration insights from a new regional deep-seismic reflection survey. In: Spencer, A.M., Embry, A.F., Gautier, D.L., Stoupakova, A.V., Sørensen, K. (Eds.), Arctic Petroleum Geology, vol. 35. Geological Society of London, Memoirs, pp. 501–508.
Lane, L., 2007. Devonian–Carboniferous paleogeography and orogenesis, northern Yukon and adjacent Arctic Alaska. Can. J. Earth Sci. 44, 679–694.
Lease, R.O., Houseknecht, D.W., Kylander-Clark, A.R.C., 2022. Quantifying large-scale continental shelf margin growth and dynamics across mid-Cretaceous Arctic Alaska with detrital zircon U-Pb dating. Geology 50, 620–625. https://doi.org/10.1130/G49118.1.
Lerand, M., 1973. Beaufort Sea. In: McCrossan, R.G. (Ed.), Future Petroleum Provinces of Canada–their Geology and Potential, vol. 1. Canadian Society of Petroleum Geologists Memoir, pp. 315–386.
Macdonald, F.A., McClelland, W.C., Schrag, D.P., Macdonald, W.P., 2009. Neoproterozoic glaciation on a carbonate platform margin in Arctic Alaska and the origin of the North Slope subterrane. Geol. Soc. Am. Bull. 121, 448–473. https://doi.org/10.1130/B26401.1.
Marín, M., Roca, E., Marcuello, A., Cabrera, L., Ferrer, O., 2021. Mesozoic structural inheritance in the cenozoic evolution of the central Catalan Coastal Ranges (western mediterranean): structural and magnetotelluric analysis in the Gaià-Montmell high. Tectonophysics 814, 1–15. https://doi.org/10.1016/j.tecto.2021.228970.
McClelland, W.C., Malone, S.J., von Gosen, W., Piepjohn, K., Laufer, A., 2012. The timing of sinistral displacement of the Pearya terrane along the Canadian Arctic margin. Z. Dtsch. Ges. Geowiss. 163, 251–259. https://doi.org/10.1127/1860-1804/2012/0163-0251.
Miall, A., 1976. Devonian geology of Banks Island, Arctic Canada, and its bearing on the tectonic development of the circum-Arctic region. Geol. Soc. Am. Bull. 87, 1599–1608.
Miller, E., Meisling A., K., Brumley, K., Coakley, B., Gottlieb, E., Hoiland, C., O'Brien, T., Soboleva, A., Toro, J., 2017. Circum-arctic lithosphere evolution (CALE) transect C: displacement of the Arctic Alaska–Chukotka microplate towards the Pacific during opening of the Amerasia Basin of the Arctic. In: Pease, V., Coakley, B. (Eds.), Circum-Arctic Lithosphere Evolution, vol. 460. Geological Society, London, pp. 57–120. Special Publications.
Moore, T.E., Box, S.E., 2016. Age, distribution and style of deformation in Alaska north of 60°N: implications for assembly of Alaska. Tectonophysics 691, 133–170. https://doi.org/10.1016/j.tecto.2016.06.025.
Moore, T.E., Dumitru, T.A., Adams, K.E., Witebsky, S.N., Harris, A.G., 2002. Origin of the Lisburne Hills-Herald Arch-Wrangel Arch structural belt: stratigraphic, structural, and fission-track evidence from the Cape Lisburne area, northwestern Alaska. In: Miller, E.L., Grantz, A., Klemperer, S.L. (Eds.), Tectonic Evolution of the Bering Shelf–Chukchi Sea–Arctic Margin and Adjacent Landmasses: Boulder, Colorado, vol. 360. Geological Society of America, pp. 77–109. Special Paper.
Moore, T.E., O'Sullivan, P.B., Potter, C.J., Donelick, R.A., 2015. Provenance and detrital zircon geochronologic evolution of lower Brookian foreland basin deposits of the western Brooks Range, Alaska, and implication for early Brookian tectonism. Geosphere 11.
Mull, C.G., Harris, E.E., Reifenstuhl, R.R., Moore, T.E., 2000. Geologic Map of the Coke Basin-Kukpowruk River Area, De Long Mountains D-2 and D-3 Quadrangles, Alaska. Alaska Division of Geological & Geophysical Surveys. https://doi.org/10.14509/2737. Report of Investigation 2000–2.
Muñoz, J.A., 1992. Evolution of a continental collision belt: ECORS-Pyrenees crustal balanced cross-section. In: McClay, K. (Ed.), Thrust Tectonics. Springer, Dordrecht, pp. 235–246.
O'Brien, T.M., Miller, E.L., Benowitz, J.P., Meisling, K.E., Dumitru, T.A., 2016. Dredge samples from the Chukchi borderland: implications for paleogeographic reconstruction and tectonic evolution of the Amerasia Basin of the Arctic. Am. J. Sci. 316, 873–924. https://doi.org/10.2475/09.2016.03.
Phillips, T.B., Jackson, C.A-L., Bell, R.E., Duffy, O.B., Fossen, H., 2016. Reactivation of intrabasement structures during rifting: A case study from offshore southern Norway. Journal of Structural Geology 91, 54–73. https://doi.org/10.1016/j.jsg.2016.08.008.
Schumacher, M.W., 2002. Upper Rhine Graben: role of preexisting structures during rift evolution. Tectonics 21, 6-1–6-17. https://doi.org/10.1029/2001TC900022.
Shaw, J.H., Hook, S.C., Sitohang, E.P., 1997. Extensional fault-bend folding and synrift deposition: an example from the Central Sumatra Basin, Indonesia. AAPG (Am. Assoc. Pet. Geol.) Bull. 81, 367–379.
Shaw, J.H., Connors, C.D., Suppe, J., 2005. Part 1, interpretation methods. In: Shaw, John H., Connors, C.D., Suppe, J. (Eds.), Seismic Interpretation of Contractional Fault-Related Folds: an AAPG Seismic Atlas, Studies in Geology #53. AAPG, Tulsa, OK, pp. 1–58.
Shephard, G.E., Muller, R.D., Seton, M., 2013. The tectonic evolution of the Arctic since Pangea breakup: integrating constraints from surface geology and geophysics with mantle structure. Earth Sci. Rev. 124, 148–183. https://doi.org/10.1016/j.earscirev.2013.05.012.
Sherwood, K.W., 1994. Stratigraphy, structure, and origin of the Franklinian, Northeast Chukchi Basin, Arctic Alaska plate. In: Thurston, D.K., Fujita, K. (Eds.), 1992 Proceedings, International Conference on Arctic Margins: United States Mineral Management Service Report No. 94-0040, pp. 245–250.
Sherwood, K.W., Craig, J.D., Lothamer, R.T., Johnson, P.P., Zerwick, S.A., 1998. Chukchi shelf assessment province. In: Sherwood, K.W. (Ed.), Undiscovered Oil and Gas Resources, Alaska Federal Offshore: United States Minerals Management Service Outer Continental Shelf Monograph MMS 98-0054, pp. 115–196.
Sherwood, K.W., Johnston, P.P., Craig, J.D., Zerwick, S.A., Lothamer, R.T., Thurston, D. K., Hurlbert, S.B., 2002. Structure and stratigraphy of the Hanna trough, US Chukchi

shelf, Alaska. In: Miller, E.L., Grantz, A., Klemperer, S.L. (Eds.), Tectonic Evolution of the Bering Shelf–Chukchi Sea–Arctic Margin and Adjacent Landmasses, vol. 360. Geological Society of America, pp. 39–66. Special Paper.

Strauss, J., Macdonald, F., Taylor, J., Repetski, J., McClelland, W., 2013. Laurentian origin for The North Slope of Alaska: implications for the tectonic evolution of the Arctic. Lithsphere 5, 477–482.

Strauss, J., Macdonald, F., McClelland, W., 2019. Pre-Mississippian stratigraphy and provenance of the North Slope subterrane of Arctic Alaska I: platformal carbonate rocks of the northeastern Brooks Range and their significance in circum-Arctic evolution. In: Piepjohn, K., Strauss, J.V., Reinhardt, L., McClelland, W.C. (Eds.), Circum-Arctic Structural Events: Tectonic Evolution of the Arctic Margins and Trans-arctic Links with Adjacent Orogens. Geological Society of America, p. 541. https://doi.org/10.1130/2018.2541(22. Special Paper.

Suppe, J., Chou, G.T., Hook, S.C., 1992. Rates of folding and faulting determined from growth strata. In: McClay, K. (Ed.), Thrust Tectonics. Springer, Dordrecht, pp. 105–121.

Tari, G., Arbounille, D., Schléder, Z., Tóth, T., 2020. Inversion tectonics: a brief petroleum industry perspective. Solid Earth 11, 1865–1889.

Tari, G., Bada, G., Beidinger, A., Csizmeg, J., Danišik, M., Gjerazi, I., Grasemann, B., Kováč, M., Plašienka, D., Šujan, M., Szafián, P., 2021. The connection between the Alps and the Carpathians beneath the Pannonian Basin: selective reactivation of Alpine nappe contacts during Miocene extension. Global Planet. Change 197, 103401. https://doi.org/10.1016/j.gloplacha.2020.103401.

Teixell, A., Labaume, P., Ayarza, P., Espurt, N., de Saint Blanquat, M., Lagabrielle, Y., 2018. Crustal structure and evolution of the Pyrenean-Cantabrian belt: a review and new interpretations from recent concepts and data. Tectonophysics 724–725, 146–170. https://doi.org/10.1016/j.tecto.2018.01.009.

Thurston, D.K., Lothamer, R.T., 1991. Seismic evidence of evaporite diapirs in the Chukchi Sea. Alaska: Geology 19, 477–480.

Thurston, D.K., Theiss, L.A., 1987. Geologic Report for the Chukchi Sea Planning Area: U. S. Minerals Management Service OCS Report, MMS 87-0046, p. 193.

Trettin, H.P., 1998. Pre-Carboniferous geology of the northern part of the Arctic Islands. Geol. Surv. Can. Bull. 425, 401.

Trettin, H.P., Mayr, U., Long, G.D.F., Packard, J.J., 1991. Cambrian to Early Devonian basin development, sedimentation, and volcanism, Arctic Islands. In: Trettin, H.P. (Ed.), Geology of the Innuitian Orogen and Arctic Platform of Canada and Greenland: Ottawa, Canada, Geological Survey of Canada, vol. 3, pp. 163–238. https://doi.org/10.4095/133959. Geology of Canada.

Villegas, E., Homza, T., Rojas, A., Tingook, R., Riobueno, F., Holroyd, J., Taylor, P., 2017. Alaska Burger prospect evaluation – insights from geochemistry (Abs). AAPG/SEG International Conference and Exhibition.

White, S.H., Green, P.F., 1986. Tectonic development of the Alpine fault zone, New Zealand: a fission-track study. Geology 14, 124–127.

Williams, G.D., Powell, C.M., Cooper, M.A., 1989. Geometry and kinematics of inversion tectonics. In: Cooper, M.A., Williams, G.D. (Eds.), Inversion Tectonics, vol. 44. Geological Society of London, pp. 3–16. Special Publications.

Wintsch, R.P., Christoffersen, R., Kronenberg, A.K., 1995. Fluid-rock reaction weakening of fault zones. J. Geophys. Res. 100 B7, 13021–13032.

Xiao, H., Suppe, J., 1992. Origin of rollover. AAPG (Am. Assoc. Pet. Geol.) Bull. 76, 509–529.